FERMILAB-PROPOSAL-0815

Scientific Spokesman:
M.H. Shaevitz
914-591-8100
Co-Spokesmen:
R.H. Bernstein
708-840-2035
S.R. Mishra
914-591-8100

Precision Measurements of Neutrino Neutral Current Interactions Using a Sign-Selected Beam FNAL Proposal P-815

T. Bolton, S.R. Mishra, P.C. Rowson, W.G. Seligman, and M.H. Shaevitz
Columbia University, New York, NY 10027

R.H. Bernstein and M. Lamm
Fermilab, Batavia, IL 60510

F.E. Taylor
Massachusetts Institute of Technology, Cambridge, MA 02139

October 9, 1990

Contents

1 Introduction **8**

1.1 Overview 8

1.2 Neutral Current Studies with a Sign-Selected Tevatron Beam 9

1.3 Physics Motivation 10

2 Experimental Method **22**

2.1 General Discussion 22

2.2 Statistical Requirements and Errors 23

2.2.1 LS Method 23

2.2.2 P-W Method 26

2.2.3 P-815 Statistical Sample and Errors 27

3 Lab E Detector and the Sign-Selected Quadrupole Triplet Beam **29**

3.1 The Lab E Detector 29

3.2 The Sign-Selected Quadrupole Triplet Beam 31

4 Experimental Systematic Errors in the Determination of $\sin^2\theta_W$ and ρ **35**

4.1 ν_e Contamination 35

4.1.1 Extraction from the Charged Current Spectrum 37

4.1.2 Extraction from Shower Shape 40

4.2 Charged-to-Neutral Current Crosstalk 43

4.3 Relative $\nu/\overline{\nu}$ Flux Uncertainties 49

4.4 Other Experimental Corrections 51

5 Theoretical Uncertainties Associated with the $\sin^2\theta_W$ Extraction 54

5.1 Charm Mass and Strange Sea Uncertainties 54

5.2 Nonisoscalar Correction 56

5.3 Electromagnetic Corrections 60

5.4 Structure Function Uncertainties 61

5.5 Non-Strange and Charmed Sea 62

6 Other Physics Topics for Phase I 63

6.1 Exclusive $\nu_\mu \rightarrow \nu_e$ Oscillation 63

6.2 Study of Wrong-sign Single Muon Production 68

7 Outline of Phase II Program 71

7.1 Phase II Goals and Plans 71

7.2 Structure Functions and QCD 72

7.3 Improvements in the Electroweak Parameter $\sin^2\theta_W$ 74

7.4 The Exclusive $\nu_\mu \rightarrow \nu_e$ Oscillation 76

7.5 Rare and New Physics 76

7.6 Beam and Detector Requirements 78

8 Requirements **80**

8.1 Phase I Detector (Lab E) Recommissioning 80

8.2 Test Beam Requirements for Phase I and R&D for Phase II 81

8.2.1 Test Beam for Phase I 81

8.2.2 Prototypes and R & D studies for Phase II 82

8.3 Costs and Requests 84

9 Conclusions **87**

List of Figures

1 The estimated precision for each measurement of $\sin^2\theta_W$ shown as a function of time. We assume the optimistic scenarios for M_W and A_{LR} discussed in the text. 16

2 The variation of the measured R_ν, M_W, and A_{LR} as a function of m_t for three values of m_H. The $\pm 1\sigma$ errors for each measurement in the late 1990's are indicated by the dotted lines 17

3 R_ν *vs.* M_W for different values of m_t. The lines (alternately solid and dotted) refer to the four top masses indicated, with full m_H variation included; errors shown are taken for the late 1990's. 20

4 Plot of R_ν and $R_{\bar{\nu}}$ *vs.* $\sin^2\theta_W$. 24

5 Contours of Constant R_ν and $R_{\bar{\nu}}$ .The dotted line is for constant $R_{\bar{\nu}} = 0.362$ and 0.368 for constant $R_\nu = 0.309$. The solid lines are for constant $R_\nu = 0.306$ and 0.3105 for constant $R_{\bar{\nu}} = 0.366$. 25

6 Schematic of the Lab E detector. The neutrino enters from the left. 30

7 A same-sign $\bar{\nu}$-induced dimuon event in the Lab E detector. Upper view is vertical, lower view is horizontal. 30

8 Layout of Proposed Sign-Selected Quadrupole Triplet. 32

9 Quadrupole Triplet Fluxes for E-744/E-770. 33

10 Sign-Selected Quadrupole Triplet Fluxes 33

11 ν_e Backgrounds in the Sign-Selected Quadrupole Triplet. 34

12 Energy Spectrum in Six Radial Bins for the QT Beam. 38

13 π/K Contamination in the QT. 39

14 Comparison of Charged-Current Data to Atherton Prediction. The boxes show the data; the points with errors are the result of the MC simulation discussed in the text. 40

15 Comparison of Charged-Current Data to Fit. The boxes show the data; the points with errors are the same simulation as above with the parameters of the Atherton fit allowed to float from the 400 GeV values. 41

16 η_3 distribution for Electromagnetic, Charged Current, and Neutral Current showers from GEANT. 42

17 η_3 Distribution for Charged and Neutral Current Events as Measured in E-744/E-770. 43

18 Fixed–Length Distribution of E-744/E-770 Data and Monte Carlo Simulation. The boxes show the data with the NC peak at small lengths; the overlay is the CC simulation. 47

19 Scaled–Length Distribution of E-744/E-770 Data and Monte Carlo Simulation. The boxes show the data in 1 counter bins with the NC peak at small lengths; the overlay is the CC simulation. 48

20 Fraction of Neutral Current Sample from Misidentified Charged Current Data. 48

21 $F_2(n)/F_2(p)$ *vs.* x. 59

22 η_3 distributions for 200 GeV $< E_{\text{calorimeter}} <$ 300 GeV and 300 GeV $< E_{\text{calorimeter}} <$ 400 GeV. Symbols represent neutral current and charged current events from the E744/E770 Quadrupole Triplet runs. Solid lines represent an EGS prediction for pure electromagnetic showers 65

23 Predicted ν_e and ν_μ Energy Spectra for the SQT. 66

24 Limits on the Exclusive Oscillation $\nu_\mu \rightarrow \nu_e$ 67

25 SQT Energy Spectrum for ν_μ CC events and $\bar{\nu}_\mu$ CC events 69

List of Tables

1 Summary of $\sin^2\theta_W$ and ρ Measurements from Neutrino-Nucleon Scattering 11

2 The Expected Error in $\sin^2\theta_W$ Prior to the Discovery of the Top Quark . . 15

3 Top Mass Limits in the Late 1990's 18

4 The Expected Error on $\sin^2\theta_W$ After the Discovery of the Top Quark. 19

5 Statistical Samples in the Proposed Experiment. 27

6 Errors in The Determinations of $\sin^2\theta_W$ and ρ. 28

7 The errors in the LS ratio and in the charm-corrected ratio R_o. 56

8 The ratio of the iron cross sections to their isoscalar counterparts using the structure function parameterization of experiment E744/E770 with $E_H > 10$ GeV. 58

9 Number of events for ν_μ-induced NC events (with CC contamination), ν_e-induced events, and expected signal for ν_e as a function of cuts. 67

10 Background to WSM with $E_{VIS} > 100$ GeV: Number of events due to $\overline{\nu}_\mu$-induced CC, ν_μ-induced $\mu^-\mu^+$, ν_e-induced $e^-\mu^+$, and ν_μ-induced NC where a μ^+ emerges in the final state, and the ν_μ-CC 70

11 The Proposed Statistical Sample in Phase II. Number of $\nu(\overline{\nu})$-induced charged current (CC), neutral current (NC), and charm-induced opposite sign dimuon ($\mu^-\mu^+$) events in the new experiment, are presented below. 72

12 Cost Estimates for P815 Upgrades (1990 US Dollars) 86

1 Introduction

1.1 Overview

We propose to initiate a new generation of neutrino physics at the Tevatron. The primary objective of this proposal (Phase I) is the precision measurement of the electroweak parameters $\sin^2\theta_W$ and ρ. Precise measurements in neutrino-nucleon scattering are valuable in their own right and provide unique windows into physics beyond the Standard Model. Each electroweak process has different dependences on new physics and an ensemble of measurements is necessary to isolate and understand new phenomena; hence results from neutrino-nucleon scattering will augment and strengthen the new data which will be available from the FNAL, SLC, and LEP colliders. In addition, this effort will extend the search for exclusive $\nu_\mu \rightarrow \nu_e$ oscillations and wrong-sign muon production.

Substantial improvements to the present measurements do not require the high flux of the Main Injector and can be accomplished with the increase provided by the new Linac. The full potential of this program will be realized with Phase II which will incorporate several improvements to the beam and apparatus. The Phase I plans and goals are presented in this proposal whereas the Phase II program is only outlined.

The advent of the Tevatron Quadrupole Triplet neutrino beam (QT) dramatically improved the available statistics and energy reach for precision measurements. With these new capabilities, the research focused on testing the Standard Model predictions with increased accuracy. Recent results by the CCFR and FMMF collaborations reveal the substantial improvements in accuracy and in the breadth of topics with the far greater statistical power of the Tevatron data. The QTB experiments have produced the most accurate measurements for many topics in the areas of structure functions, dilepton production, and inverse muon decay. Searches for new phenomena have led to stringent limits on right handed currents, like-sign dimuon production, and iso-singlet type heavy neutral leptons.

Improvements over the present E744/E770/E733 data sets can be made in three areas: (1) improvements in the beam, (2) an increase in the event sample, and (3) new detector capabilities with lower systematic uncertainties. An increase of statistics has in the past seemed particularly difficult since the two previous runs were very productive. With the Main Injector Upgrade, however, more than an order of magnitude increase is expected which has precipitated interest in continuing the neutrino program. The effort described in this proposal incorporates the three improvements mentioned above in two phases. For Phase I, to be run in the next fixed target period, the beam will be improved by sign-selecting the parent mesons thereby separating neutrinos and antineutrinos. Prototypes of detector improvements for Phase II will be studied during the run.

1.2 Neutral Current Studies with a Sign-Selected Tevatron Beam

The QT beam is inadequate for precise electroweak experiments. Due to the lack of sign selection, the beam is a mixture of neutrinos and antineutrinos in a ratio of about two to one. Separate measurements of $R_\nu = \sigma^\nu_{NC}/\sigma^\nu_{CC}$ and $R_{\bar{\nu}} = \sigma^{\bar{\nu}}_{NC}/\sigma^{\bar{\nu}}_{CC}$ are therefore not possible and the extraction of the Standard Model ρ parameter cannot be made. In addition, the main experimental background from ν_e's and $\overline{\nu_e}$'s in the neutrino beam is enhanced by the K_L component in the secondary beam. This component is especially troublesome since the production of K_L's is not precisely known and could contribute an error to the measured $\sin^2\theta_W$ of up to $\pm.005$. Hence we propose a new Sign-Selected Quadrupole Triplet beam (SQT) be constructed. The new beam would allow the separate measurements of R_ν and $R_{\bar{\nu}}$ with little contamination from the opposite species, and would remove the ν_e background from K_L decays.

During the Fall '92 running period, we plan to split the time between neutrinos and antineutrinos and collect data corresponding to 10^{18} POT for each type. This data sample will then include 650K CC_ν, 110K $CC_{\bar{\nu}}$, 200K NC_ν, and 42K $NC_{\bar{\nu}}$ in the Lab E fiducial volume after radius and hadron energy cuts appropriate for the neutral current analysis.

This represents a factor of *four and one-half* increase in neutral current event statistics for ν and a factor of *twenty* for $\bar{\nu}$ induced events over the previous best measurement of CDHS. In addition, the new data sample will have a much higher mean energy than the older CDHS data, which will reduce the systematic uncertainties due to charm mass effects and the charged current contamination in the neutral current sample. These systematic uncertainties dominated the final errors of the previous measurements.

The large sample of $\bar{\nu}$ NC events that will be available from the P815 experiment will allow the measurement of the Paschos-Wolfenstein variables, $R^{\pm} = (\sigma^{\nu}_{NC} \pm \sigma^{\bar{\nu}}_{NC})/(\sigma^{\nu}_{CC} \pm \sigma^{\bar{\nu}}_{CC})$. These variables are less sensitive to certain systematic uncertainties; for example, R^{-} has little dependence on the charm quark mass making possible a precise measurement of $\sin^2 \theta_W$. Precise measurements of $R^{\pm}$ have not been presented previously due to the meager $\bar{\nu}$ data available. A comparison of the expected errors for P815 with the published results of CDHS, CHARM, and CCFR is given in the Table below.[1] The charm mass error for each of the experiments corresponds to $\delta m_c = 0.25$ GeV which is the expected uncertainty that will be obtained from the E744/E770 dimuon analysis in 1991.

1.3 Physics Motivation

Studies of neutral current phenomena are currently the best area to probe the Electroweak Standard Model both for consistency and for new physics. Since the top quark mass is large, the electroweak radiative corrections have become a new tool for probing the model. These investigations have led to restrictions on the top quark mass and other new physics from comparisons of measurements of different processes through the differing radiative corrections.

Table 1: Summary of $\sin^2\theta_W$ and ρ Measurements from Neutrino-Nucleon Scattering

Parameter	Experiment	Statistical Error	Systematic Error	Charm Mass Error	Total Error
$\sin^2\theta_W$	P-815	0.0017	0.0022	0.0006	0.0029
	CDHS	0.0041	0.0036	0.0033	0.0064
	CHARM	0.0043	0.0040	0.0030	0.0066
	CCFR	0.0080	0.0052	0.0030	0.0110
ρ	P-815	0.0019	0.0029	0.034	0.0049
	CDHS	0.0200	0.0097	0.0057	0.0230
	CHARM	0.0180	-	-	-
	CCFR	0.0180	0.0148	0.0060	0.0240

Within the context of the minimal Standard Model, the largest uncertainties in higher order calculations arise from our ignorance of the top quark and Higgs boson masses. The current best limits or estimates of the top quark mass come mainly from comparisons of R_ν and the mass of the Z. A comparison of the W and Z boson masses is also sensitive to the top quark mass but the comparison is currently restricted by the imprecision of the W-boson mass measurement. Lower mass limits on m_t and m_H are available directly from experiments at the Tevatron and from LEP respectively, while indirect upper limits have been inferred from both experimental data and theoretical argument. The present state of our knowledge is given approximately by

$$90 \text{ GeV} < m_t < 250 \text{ GeV} \quad \text{and} \quad 45 \text{ GeV} < \mathrm{m_H} < 1000 \text{ GeV} . \tag{1.3.1}$$

New measurements of the forward-back asymmetries at LEP and a better W-boson mass measurements from LEP II and CDF/D0 will become competitive with the R_ν measurement in the next few years but a precise measurement of R_ν will stand as an important check of the model. An improvement in the neutrino $\sin^2\theta_W$ measurement from the current 3% error to our proposed 1.3% error would allow the top mass restriction to be improved; when combined with the other electroweak measurements it will offer precision tests of the Standard Model as well. In addition, the new measurement of ρ will be of a sufficient accuracy to probe the Standard Model for indications of new physics.

The tree level value of any weak parameter dependent measureable quantity, such as M_W, $\sin^2\theta_W$, the forward-backward charge asymmetries (A_{FB}) or R_ν, is modified by loop diagrams containing, in particular, top quarks and Higgs bosons. The dependence of these corrections on the constituent masses is roughly quadratic in m_t and logarithmic in m_H. Hence top quark effects usually dominate despite the much larger mass range allowed for the Higgs boson. Due to the critical role played by the top quark mass uncertainty, we can distinguish two "eras" in electroweak physics :

- **Prior** to the observation of top: at least two measurables are needed to constrain the Standard Model, in particular the ranges of m_t and m_H.

- **After** the precise measurement of m_t—errors of order ± 5GeV may be achievable at the Tevatron for $m_t \approx 150$ GeV—the observables R_ν and A_{LR} will test the overall consistency of the Standard Model and probe for new physics.[2].

We will consider both scenarios in what follows, but we will assume that the top mass will not be directly measured until the mid 1990's at the earliest.

It is possible to treat the top and Higgs masses as parameters of the Standard Model, along with the very accurately determined parameters α, G_F and M_Z, and to express each measurable separately as a function of m_t and m_H. However, it is conventional to reinterpret all measurables in terms of an appropriately defined weak mixing angle, in order to simplify direct comparisons of the different experimental quantities. In order to standardize our discussion, we will express all measurements in terms of the "Sirlin" definition of the weak mixing angle[3] given by :

$$sin^2\theta_W = 1 - (\frac{M_W}{M_Z})^2, \tag{1.3.2}$$

but our results could just as well be cast in terms of $\sin^2\theta^*_W$ defined from weak asymmetries on the Z resonance, for example. Another useful definition is $\sin^2\bar{\theta}_W$, the weak mixing angle as defined in terms of the coupling at the Z-pole. This definition is particularly important in studying deviations of ρ from Standard Model predictions. With the advent of a new level of precision in electroweak measurements it is essential to standardize one's definition of $\sin^2\theta_W$ due to the different dependence of each defined weak mixing angle on higher order effects.

We have studied the dependence of several electroweak measurables on the top quark and Higgs boson loop effects. A general purpose electroweak corrections program written by M. Peskin has been used for these studies[4]. The magnitude of the variation of the top quark loop correction as a function of m_t can be seen to be dependent on the the central value of m_t that is chosen (in general, the top mass effects are larger for larger top masses).

In our estimation of higher-order effects we allow both the top quark and Higgs boson

masses to vary over the full range given above (Eq. 1.3.1) to deduce the variation expected from the Standard Model for a given measurable. We take $m_t = 150$ GeV and $m_H = 100$ GeV to define our central value[5]. The estimated total experimental error for a given measurable is then translated into an error in the determination of the chosen weak parameter ($\sin^2\theta_W$ or m_t, for example).

In order to map out the progress of high precision electroweak measurements during the coming decade, we have constructed a probable timetable of results from e^+e^- colliders and the CDF/D0 experiments along with an estimate of our own future progress in Table 2. The LEP and SLC results contained in the table are based on the following optimistic assumptions[6] :

1. The SLC will have produced 100,000 Z events with 40% electron beam polarization by 1993. This performance is extrapolated to 300,000 events in 1995. Results for event samples of 10^6 also are given in case LEP is eventually run with longitudinally polarized beams.

2. The LEP experiments will have 200pb^{-1} or 6×10^6 Z events by 1993-94.

3. LEP II will collect 500pb^{-1} during the three year period from 1994-1996.

4. LEP luminosity will be upgraded to produce $\mathcal{O}(10^6)$ Z events during the period 1998-1999.

Note that for the neutral current measurement, the Paschos-Wolfenstein variable R^-, rather than R_ν, will be used once high statistics ν and $\overline{\nu}$ data are available.

The errors shown are estimated by including both experimental and electroweak correction uncertainties as explained above and are rounded off to the nearest 0.0005. A graphical statement of the quoted errors of Table 3 is given in Figure 1. Here we plot the sensitivity of the A_{LR}, M_W and R_ν/R^- measurements to $\sin^2\theta_W$ as a function of measurement precision.

Table 2: The Expected Error in $\sin^2\theta_W$ Prior to the Discovery of the Top Quark

	early 1990's	mid 1990's	late 1990's
	'94 ($\delta = 150$ MeV)	'95 ($\delta = 100$ MeV)	'96 ($\delta = 70$ MeV)
M_W	0.003	0.002	0.0015
	'93 ($N_Z = 10^5$)	'95 ($N_Z = 3 \times 10^5$)	? ($N_Z = 10^6$)
A_{LR}	0.004	0.003	0.002
	'94 (200pb^{-1})		'99 (2000pb^{-1})
A_{FB}^b	0.004		0.003
	'92 (sys.limit)		
Γ_{ll}	0.005		
	'91 (1% R_ν)	'94 (1.2% R^-)	'97 (0.4%/0.6% R_ν/R^-)
R_ν/R^-	0.005	0.003	0.0015

m_t,m_H effects are included.

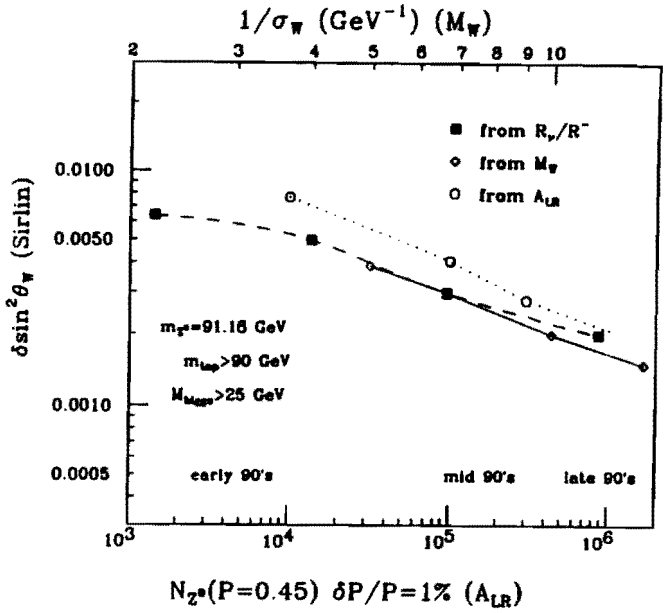

Figure 1: The estimated precision for each measurement of $\sin^2\theta_W$ shown as a function of time. We assume the optimistic scenarios for M_W and A_{LR} discussed in the text.

The m_t and m_H dependence of R_ν, M_W and A_{LR} are shown in figure 2, along with the experimental errors expected by the late 1990's. From these calculations it is possible to deduce upper and lower limits on m_t from each measurable which we give in Table 3.

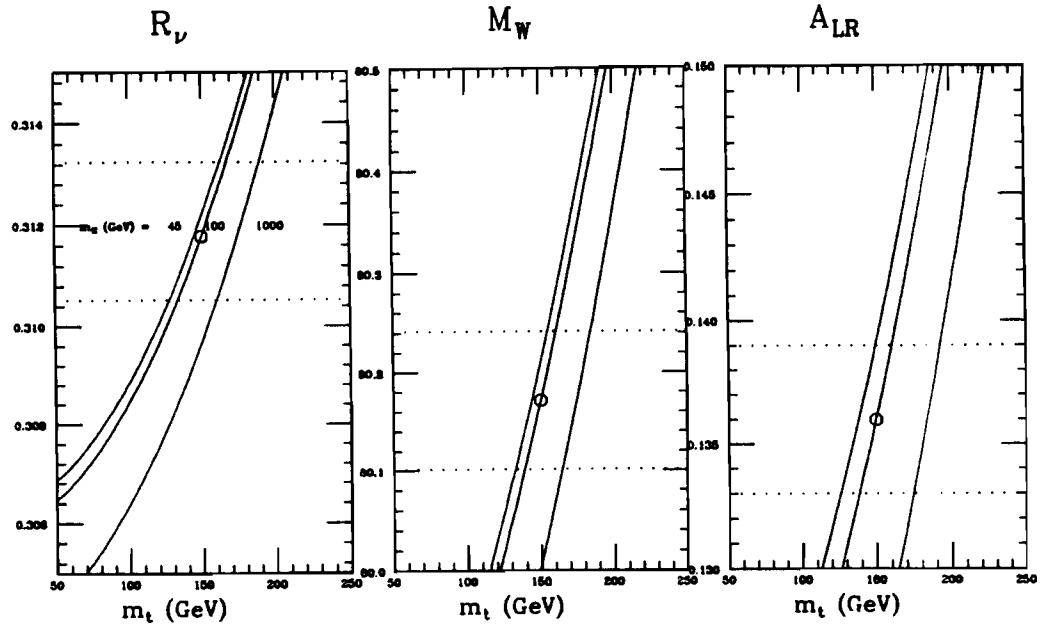

Figure 2: The variation of the measured R_ν, M_W, and A_{LR} as a function of m_t for three values of m_H. The $\pm 1\sigma$ errors for each measurement in the late 1990's are indicated by the dotted lines.

The contents of Table 2 are modified if one allows for the observation of top and the accurate measurement of the top mass by CDF and D0, due to the subsequent reduction in the uncertainties of the electroweak corrections. If, for example, we consider the optimistic scenario where $m_t = 150 \pm 10$ GeV is known by 1995, we will have the situation shown in Table 3. The sensitivity of A_{LR} to the top mass is evident. We will discuss the similar dependence of $R_{\bar{\nu}}$ shortly.

Up to now, we have discussed neutrino-nucleon scattering as a "stand-alone" measurement which provides valuable information about the Standard Model. However, much of the power of neutral current measurements from DIS-ν scattering becomes apparent when compared with data from the e^+e^- and hadron colliders. This follows from the different dependence on radiative corrections of R_ν relative to M_W or the observables from the Z pole. In Figure 3, we illustrate how R_ν and M_W together can significantly narrow the range

Table 3: Top Mass Limits in the Late 1990's

	top mass range (GeV)
M_W	130—185
A_{LR}	125—195
R_ν	130—190

The $\pm 1\sigma$ m_t range from several different measurements :
full m_H effects included.

of unknown electroweak parameters.

While R_ν is quite sensitive to $\sin^2\theta_W$, and relatively insensitive to m_t, exactly the reverse is true of $R_{\overline{\nu}}$. This fact is readily apparent when the relationship between the the measureables R_ν or $R_{\overline{\nu}}$ and the derived quantities $\sin^2\bar{\theta}_W$ and ρ, the neutral current strength parameter. The ρ parameter should be equal to 1 in the single doublet Higgs minimal Standard Model, if one ignores the electroweak corrections due to the heavy top quark and Higgs boson. Hence, in being particularly sensitive to ρ, $R_{\overline{\nu}}$ is particularly sensitive to the m_t radiative corrections and to more complex Higgs structure. Following the approximate treatment due to Rosner[7], we can express the top mass dependence of $\rho - 1 = \Delta\rho$ as

$$\Delta\rho_t \approx \frac{3\alpha}{16\pi \sin^2\bar{\theta}_W}(\frac{m_t}{M_W})^2, \tag{1.3.3}$$

which predicts a deviation of ρ from 1 equal to $+0.007$ for $m_t = 150$ GeV. Here we have defined

$$\sin^2\bar{\theta}_W = 1 - \frac{M_W^2}{\rho M_Z^2} \tag{1.3.4}$$

which is the weak mixing angle defined at the Z-pole. The Higgs boson corrections are

Table 4: The Expected Error on $\sin^2\theta_W$ After the Discovery of the Top Quark.

	mid 1990's	late 1990's
	'95 ($\delta = 100$ MeV)	'96 ($\delta = 70$ MeV)
M_W	0.002	0.0015
	'95 ($N_Z = 3 \times 10^5$)	? ($N_Z = 10^6$)
A_{LR}	0.0015	0.0015
	'94 (0.6%)	'97 (0.4%)
R_ν	0.003	0.0015

The expected error on $\sin^2\theta_W$ from several different electroweak measurements : m_t,m_H effects included, $m_t = 150 \pm 10$ GeV.

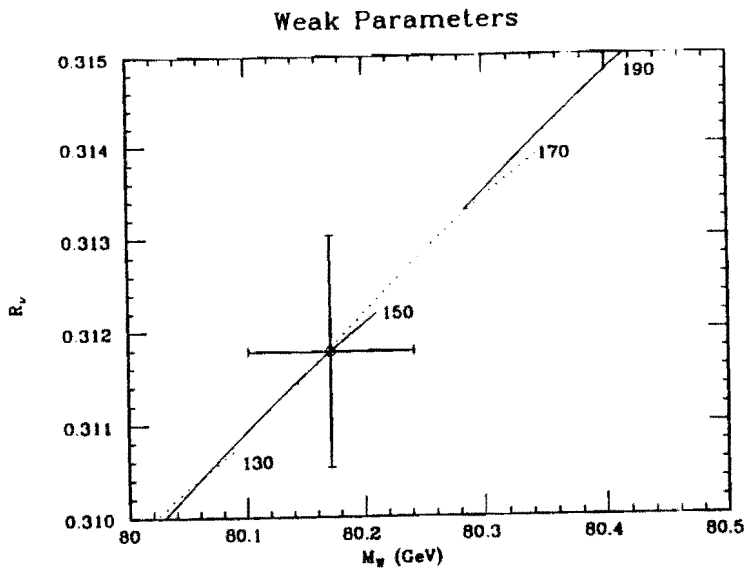

Figure 3: R_ν *vs.* M_W for different values of m_t. The lines (alternately solid and dotted) refer to the four top masses indicated, with full m_H variation included; errors shown are taken for the late 1990's.

logarithmic in the Higgs mass and opposite in sign to those of m_t; these effects are also relatively small, and are approximately -0.0024 for $m_H = 1000$ GeV. The effect of a triplet Higgs can be of either sign, and will depend on the relative magnitudes of the various triplet Higgs vacuum expectation values, and can be comparable in magnitude to the top mass effects. With our proposed measurement precision for ρ of less than 0.5%, we will be sensitive to electroweak radiative effects and to new physics.

A precise measurement of $R_{\overline{\nu}}$ would allow one to probe the Higgs sector with greater sensitivity relative to the R_ν measurement once the top mass was measured. This feature of the antineutrino measurement nicely complements the power of R_ν in the early years of the this decade.

To summarize, our proposed neutrino and anti-neutrino neutral current experiment should make the following contributions to our understanding of electroweak physics :

- The R_ν and R^- measurements will determine $\sin^2\theta_W$ to a precision comparable to that available from the collider experiments.
- Due to differences in sensitivity to radiative corrections, when combined with data from the colliders, neutrino and anti-neutrino neutral current measurements will provide powerful constraints on the Standard Model.
- The antineutrino data will be sensitive to new physics embodied in the parameter ρ.

2 Experimental Method

2.1 General Discussion

Deep-inelastic neutrino-nucleon scattering yields data which allow several methods of determining $\sin^2\theta_W$ and ρ. All are founded on the electroweak couplings of the Z^0 boson with quarks which depend on the weak isospin, T_3^i, and electric charge, Q^i, of the quarks, and on $\sin^2\bar{\theta}_W$ by the relation:

$$\delta^i = T_3^i - Q^i \sin^2\bar{\theta}_W \tag{2.1.1}$$

The ρ parameter, defined by the relation,

$$\rho = M_W^2/M_Z^2\cos^2\bar{\theta}_W \tag{2.1.2}$$

measures the strength of the neutral current interaction. In the standard model with only one Higgs doublet, $\rho = 1$. Beyond the tree level, ρ can be different from one depending on various electroweak corrections as a function of the top quark mass, m_{top}, among other parameters. The parameter $\sin^2\theta_W$ measured in deep-inelastic scattering is numerically close to the Sirlin value.[8] In the following discussion we shall treat $\sin^2\theta_W$ and ρ derived from DIS as empirical parameters which will ultimately be realted to $\bar{\theta}_W$, θ_W of Sirlin, *etc.*

Llewellyn Smith[9] has shown that for an isoscalar target with only massless u and d quarks, isospin invariance can be used to determine the largest contributions to the neutral current (NC) and charged current (CC) cross sections. Thus, the ratio $R_\nu = NC/CC$ can be written as:

$$R_{\nu(\bar{\nu})} = \rho^2(1/2 - \sin^2\theta_W + 5/9\sin^4\theta_W(1 + r^{(-1)})), \tag{2.1.3}$$

where $r = \sigma_{\bar{\nu}}^{CC}/\sigma_\nu^{CC}$ is the ratio of the antineutrino to neutrino charged-current cross section with the same experimental cuts as are used in the $\sin^2\theta_W$ analysis. The factor r,

derived from measurement, absorbs many of the quark-parton corrections which are otherwise difficult to take into account. In this method, (referred to here as the LS method), the corrections associated with the target being nonisoscalar, the strange quark contribution, the charm quark kinematic factors ,etc. are all treated as small corrections. An alternative method is to compute the NC/CC ratio directly from the quark-parton model using a parameterization of the quark structure functions. Unless all of the measurement correlations are included this calculation leads to a greater sensitivity to the experimental errors.

Another method for determining $\sin^2\theta_W$ which is theoretically robust is derived from the Paschos -Wolfenstein[10] (P-W) relations:

$$R^- = \frac{(\sigma_\nu^{NC} - \sigma_{\overline{\nu}}^{NC})}{(\sigma_\nu^{CC} - \sigma_{\overline{\nu}}^{CC})} = \rho^2(\frac{1}{2} - \sin^2\theta_W) \tag{2.1.4}$$

$$R^+ = \frac{(\sigma_\nu^{NC} + \sigma_{\overline{\nu}}^{NC})}{(\sigma_\nu^{CC} + \sigma_{\overline{\nu}}^{CC})} = \rho^2(\frac{1}{2} - \sin^2\theta_W + \frac{10}{9}\sin^4\theta_W) \tag{2.1.5}$$

Most corrections tend to cancel in the R^- ratio which makes the extracted $\sin^2\theta_W$ insensitive to many of the theoretical uncertainties. However, the relative normalization of neutrino to antineutrino data is required in order to obtain $\sin^2\theta_W$. Previous experiments have not used the P-W method due to these normalization uncertainties combined with inadequate antineutrino statistics. For the P815 experiment, the high statistics combined with accurate techniques for determining the relative flux indicate that the P-W method will give the smallest error on $\sin^2\theta_W$.

2.2 Statistical Requirements and Errors

2.2.1 LS Method

Using the Lleweylln Smith formulation, we estimate the precision required in a measurement of $\sin^2\theta_W$ in the range of $\pm 1\%$. In Fig. 4 R_ν and $R_{\bar{\nu}}$ are plotted as a function of $\sin^2\theta_W$ for fixed $r = 0.42$. We note that R_ν is much more sensitive to $\sin^2\theta_W$ than is $R_{\bar{\nu}}$, and as is

well known the neutrino NC/CC ratio is much more efficacious in determining $\sin^2\theta_W$ than is the antineutrino ratio. Numerically we find for neutrinos $\delta \sin^2\theta_W \approx -1.5R_\nu$, but for antineutrinos $\delta \sin^2\theta_W \approx -18\delta R_{\bar{\nu}}$ for $\sin^2\theta_W$ in the region of 0.23.

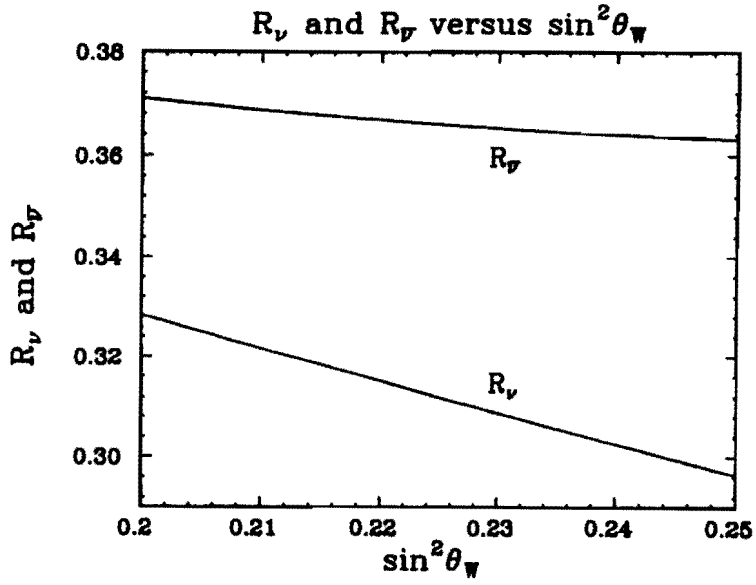

Figure 4: Plot of R_ν and $R_{\bar{\nu}}$ *vs.* $\sin^2\theta_W$.

The statistical precision in determining R_ν and $R_{\bar{\nu}}$ is given convienently by

$$\frac{\delta R_\nu}{R_\nu} = \frac{2.1}{\sqrt{CC(\nu)}} \tag{2.2.6}$$

$$\frac{\delta R_{\bar{\nu}}}{R_{\bar{\nu}}} = \frac{1.9}{\sqrt{CC(\bar{\nu})}} \tag{2.2.7}$$

where $CC(\nu)$ and $CC(\bar{\nu})$ are the numbers of observed neutrino and antineutrino charged-current events. To know R_ν or $R_{\bar{\nu}}$ to $\pm 0.4\%$ requires an exposure of about 250K CC events. A similar analysis can be used to estimate the number of events needed to achieve a given statistical precision of $\sin^2\theta_W$ using only the neutrino ratio (assuming that ρ is given by the standard model). We find the number of CC(ν) events needed to achieve a given error $\delta \sin^2\theta_W$ is $CC(\nu) \approx 10(R_\nu/\delta(\sin^2\theta_W))^2$. Thus an exposure of 250K CC(ν) events would result in a statistical error $\delta \sin^2\theta_W \approx \pm 0.002$. Accumulating 250K CC($\bar{\nu}$) events would

result in $\delta\rho = \pm 0.002$. A massive calorimeter in an intense neutrino beam can collect up to 10^6 events which would correspond to a $\pm 0.5\%$ statistical error in $\sin^2\theta_W$.

An analysis of both R_ν and $R_{\bar{\nu}}$ is necessary to determine $\sin^2\theta_W$ and ρ. In Fig. 5, we plot the contours of constant R_ν and $R_{\bar{\nu}}$ in ρ–$\sin^2\theta_W$ space using Eq 2.1.3. Note that the constant $R_{\bar{\nu}}$ contour is almost independent of $\sin^2\theta_W$ as discussed above, whereas both $\sin^2\theta_W$ and ρ vary along the corresponding neutrino contour. The intersection of the two contours determines $\sin^2\theta_W$ and ρ. To analyze the errors in a simultaneous determination of $\sin^2\theta_W$ and ρ, we refer to Fig. 5 where the intersection region of several contours of R_ν and $R_{\bar{\nu}}$ is shown.

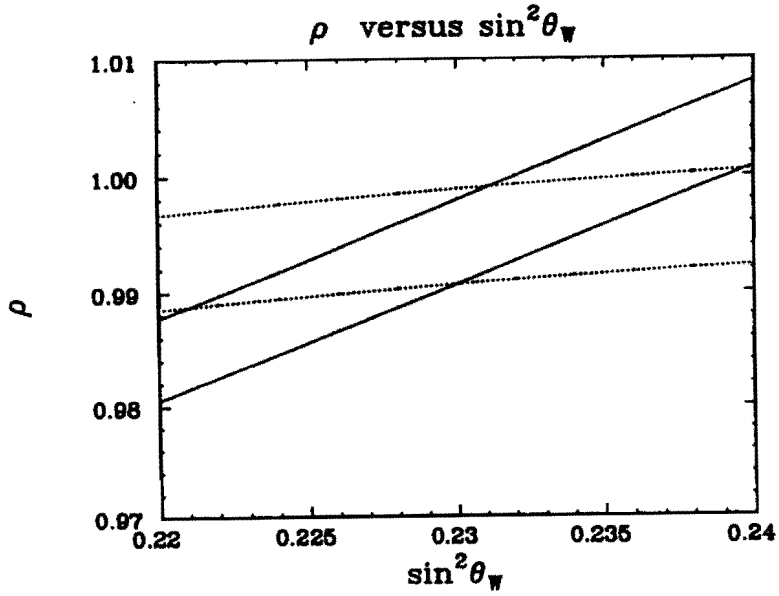

Figure 5: Contours of Constant R_ν and $R_{\bar{\nu}}$ .The dotted line is for constant $R_{\bar{\nu}} = 0.362$ and 0.368 for constant $R_\nu = 0.309$. The solid lines are for constant $R_\nu = 0.306$ and 0.3105 for constant $R_{\bar{\nu}} = 0.366$.

For $\sin^2\theta_W(\rho)$ in the region of 0.230 (0.995) and treating the neutrino and antineutrino as uncorrelated measurements (which they are statistically), we find numerically:

$$\delta \sin^2\theta_W = \left[(1.75\delta R_\nu)^2 + (1.45\delta R_{\bar{\nu}})^2\right]^{\frac{1}{2}} \qquad (2.2.8)$$

and

$$\delta\rho = \left[(0.20\delta R_\nu)^2 + (1.50\delta R_{\bar{\nu}})^2\right]^{\frac{1}{2}} \tag{2.2.9}$$

Thus when R_ν and $R_{\bar{\nu}}$ are used to simultaneously determine $\sin^2\theta_W$ and ρ we find that the precision requirements of both the neutrino and anti-neutrino NC/CC ratios are equally stringent. The parameter ρ is determined mostly from the measurement of $R_{\bar{\nu}}$ as indicated above. An analysis of this kind argues that a considerable exposure be given to antineutrinos.

2.2.2 P-W Method

In the P-W method, R^- dominates the determination of $\sin^2\theta_W$ and R^+ that of ρ. Quantitatively, $\delta\sin^2\theta_W \approx -\delta R^-$ and $\delta\sin^2\theta_W \approx -2\delta R^+$ for $\sin^2\theta_W \approx 0.23$. Since, as will be shown in subsequent sections, the errors, δR^+ and δR^-, are comparable, the best determination of $\sin^2\theta_W$ is obtained by statistically combining the R^+ and R^- measurements under the standard model assumption with ρ fixed. The error in $\sin^2\theta_W$ is then given by:

$$\delta\sin^2\theta_W = \left(\frac{1}{(\delta R^-)^2} + \frac{1}{(2\delta R^+)^2}\right)^{-\frac{1}{2}} \approx 0.9\ \delta R^-$$

For the extraction of ρ and $\sin^2\theta_W$, both R^+ and R^- are used. The estimated error on ρ and $\sin^2\theta_W$ by this procedure is:

$$\delta\rho \approx 1.5\ ((\delta R^+)^2 + (.5\delta R^-)^2)^{\frac{1}{2}}$$

$$\delta\sin^2\theta_W \approx \left((1.42\delta R^+)^2 + (1.71\delta R^-)^2\right)^{\frac{1}{2}}$$

Although it will be shown that the expected error on $\sin^2\theta_W$ from the P-W method will be less than the LS method, the two methods are complementary. The LS method has a smaller statistical error but is much more sensitive to the theoretical uncertainties, especially the charm quark mass. On the other hand, the P-W method has a larger statistical error and an intrinsic sensitivity to uncertainties in the relative flux. R^- has the further advantage of a smaller sensitivity to the $CC \rightarrow NC$ subtraction since the effect of the contamination

tends to cancel in the difference of cross-sections. However, we believe that a strength of the proposed program will be the ability to use the different techniques as checks on systematic uncertainties.

2.2.3 P-815 Statistical Sample and Errors

For both the LS and P-W methods, ratios of numbers of charged and neutral current events are formed after the application of experimental cuts. From our previous studies with the Lab E detector, we have determined that a $E_{had} > 10$ GeV cut will allow good trigger efficiency and calorimetry for both neutral and charged current events. We would also plan to use fiducial volume cuts that incorporate 75% of the target calorimeter longitudinally with a transverse radius cut of 1 meter. (The transverse size of the target is a square 3m by 3m.) With these cuts the proposed 1993 fixed target run of 2×10^{18} POT split equally between neutrinos and antineutrinos would yield the data sample given in the table below:

Type	No. of Events
ν CC	650,000
ν NC	200,000
$\overline{\nu}$ CC	110,000
$\overline{\nu}$ NC	42,000

Table 5: Statistical Samples in the Proposed Experiment.

The estimated statistical errors for the various derived quantities are shown in Table 6 on the next page along with the systematic uncertainties that will be described in the subsequent sections. The values of R_ν and $R_{\overline{\nu}}$ listed under the LS method are the corrected values, i.e. $R_\nu^{LS} = R_\nu - \frac{5}{9} r \sin^4\theta_W$ and $R_{\overline{\nu}}^{LS} = R_{\overline{\nu}} - \frac{5}{9}(1/r)\sin^4\theta_W$.

Contribution	LS Method				P-W Method			
	$\frac{\delta R_\nu}{R_\nu}$ (%)	$\frac{\delta R_{\bar{\nu}}}{R_{\bar{\nu}}}$ (%)	$\delta \sin^2\theta_W$	$\delta\rho$ (%)	$\frac{\delta R^-}{R^-}$ (%)	$\frac{\delta R^+}{R^+}$ (%)	$\delta \sin^2\theta_W$	$\delta\rho$ (%)
Statistical Error	.26	.57	.0013	.28	.71	.25	.0017	.19
Experimental Errors								
CC $\rightarrow$ NC	.46	.24	.0023	.12	.74	.37	.0017	.24
NC $\rightarrow$ CC	.10	.10	.0005	.05	.10	.10	.0003	.05
ν_e Contamination	.16	.07	.0008	.04	.16	.11	.0004	.06
WBB Subtraction	$< .01$	$< .01$	—	—	$< .01$	$< .01$	—	—
Cosmic Ray Subtr.	.01	.05	.0001	.03	.12	.05	.0003	.03
Relative Flux	.06	.34	.0003	.17	.53	.06	.0012	.11
$(\phi_\nu/\phi_{\bar{\nu}} \pm 1.5\%)$								
Total Experimental	.50	.44	.0025	.22	.94	.40	.0022	.27
Theoretical Errors								
Strange Sea	.09	.22	.0004	.11	.01	.11	.0001	.06
$(\kappa = .49 \pm .06)$								
Long. Stucture	.01	.03	.0001	.02	.03	.09	.0001	.05
Function ($\pm 20\%$)								
Non-Isoscalarity	.11	.05	.0006	.03	.20	.06	.0005	.05
$(\frac{U_V}{D_V} \pm 10\%)$								
Quark Sea	.01	.09	.0001	.05	.04	.01	.0001	.01
$(\frac{(\bar{U}+\bar{D})}{(U+D)} \pm 10\%)$								
Charm Sea	.03	.06	.0001	.03	.03	.03	.0001	.02
$(\frac{C}{S} = .05 \pm .05)$								
Radiative Effects	.12	.20	.0006	.10	.16	.14	.0003	.08
$(Corr. \pm 10\%)$								
Total Theoretical	.17	.32	.0009	.16	.25	.21	.0006	.12
Charm Mass	.56	1.17	.0028	.58	.18	.66	.0004	.34
$(m_c = 1.35 \pm .25 GeV)$								
Total Error	.81	1.41	.0040	.70	1.22	.84	.0029	.49

Table 6 Errors in The Determinations of $\sin^2\theta_W$ and ρ.

3 Lab E Detector and the Sign-Selected Quadrupole Triplet Beam

3.1 The Lab E Detector

The Phase I experiment will be performed with the recommissioned Lab E detector. The Lab E detector consists of two parts: a high density target calorimeter followed by a toroidal muon spectrometer (see Fig. 6). The 690 ton target calorimeter (dimensions 3.1 × 3.1 × 16.5 m^3) is instrumented with liquid scintillation counters separated by 10 cm of steel and drift chambers separated by 20 cm of steel. The calorimeter has a RMS resolution of $\delta E/E = .89/\sqrt{E(GeV}$. The muon spectrometer contains three iron toroidal magnets (total transverse momentum kick of 2.4 GeV/c), drift chambers for muon tracking, and acrylic counters for event triggering and timing. The muon momentum resolution is $\delta P/P$=11%. The output of the target and toroid scintillation counters is read into a buffered ADC system. The drift chamber system in the toroid consists of five banks of five drift chambers each with no material between chambers in a given bank. Two of the drift chamber banks are located 3m and 7m downstream of the toroids in order to increase the lever arm for measuring muon momentum. The drift chambers have an intrinsic resolution of 250 μm and are read out by a multi-hit TDC system which has a precision of 4 ns. The scintillation counters in the target and the toroid are also read out by the TDC system. The timing information from the counters enables us to measure the event interaction time with a resolution of 5 ns.

Fig. 7 shows an event display of a same-sign dimuon in the Lab E detector during the 1985 run. The histogram on the event display shows pulse height in calorimeter counters. The curves represent fitted muon tracks using drift chamber hits in the calorimeter and toroid spectrometer. The muon momenta are 46 and 33 GeV/c at the vertex; the measured hadron energy is 70 GeV.

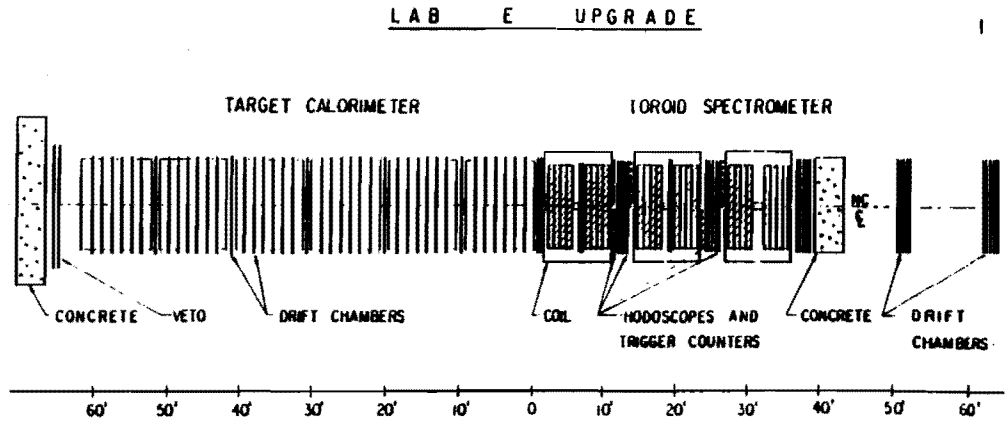

Figure 6: Schematic of the Lab E detector. The neutrino enters from the left.

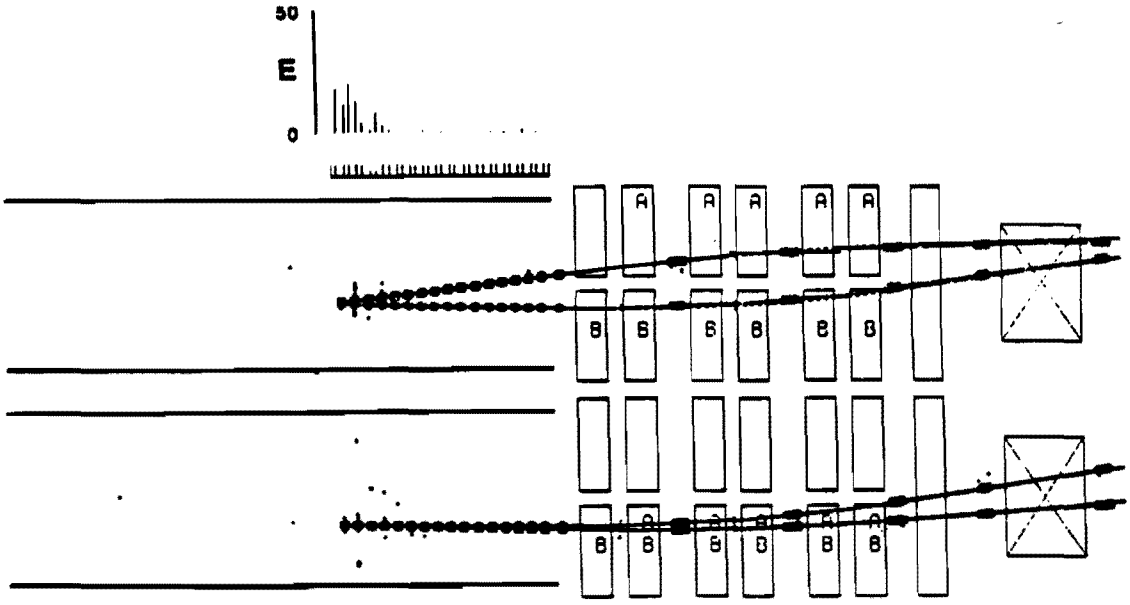

Figure 7: A same-sign $\bar{\nu}$-induced dimuon event in the Lab E detector. Upper view is vertical, lower view is horizontal.

3.2 The Sign-Selected Quadrupole Triplet Beam

The sign-selected quadrupole triplet beam (SQT) is the key to reducing backgrounds and achieving adequate statistics. It also makes possible the important physics goal of measuring ρ^2 and $\sin^2\theta_W$ separately. Wide-band beams such as the Quadrupole Triplet (QT) do not separate ν from $\bar{\nu}$ and have a significant flux of ν_e from K_L, which, as we explained earlier, yield an unacceptable error. On the other hand, high-energy dichromatic beams provide pure nuetrino/antineutrino fluxes but suffer from low flux. The SQT provides the sign-separation and K_L rejection of dichromatic beams with an acceptable loss of flux. We describe the beam in this Section and quote expected rates and spectra.

Fig. 8 shows the layout of the proposed beam. We target primary protons at 6.8 mr and bend along a Quadupole Triplet line which focuses 400 GeV secondaries.[11] The neutrals are thus pointed 6.8 mr away from the detector before they pass through the train. A final dipole increases the bend so that remaining neutrals are pointed at almost 10 mr from the detector. The target must be moved 10 m. upstream of its present location which requires removing several dipoles just upstream of the target. This implies that while we may run *either* neutrino or antineutrino mode within a given run, restoring QT operation will require waiting for a shutdown.

The primary proton beam stops in the second beam dump for neutrino running. To switch to antineutrino mode one reverses all the magnet currents (while leaving the primary proton targeting unaltered) and the protons then stop in the first dump. A small adjustment to the field of the final dipole will be made to center the lower energy negatives on the detector.

Restoring a Quadrupole Triplet line is accomplished in three steps: (1) first the train is brought back to its old location , (2) the upstream dipoles are replaced, and (3) within the train, the two dipoles are turned off and the protons are targeted at 0 mr. The protons then dump after the end of the decay pipe in the current location.

We have checked the rates used in this Proposal carefully against the QT fluxes from

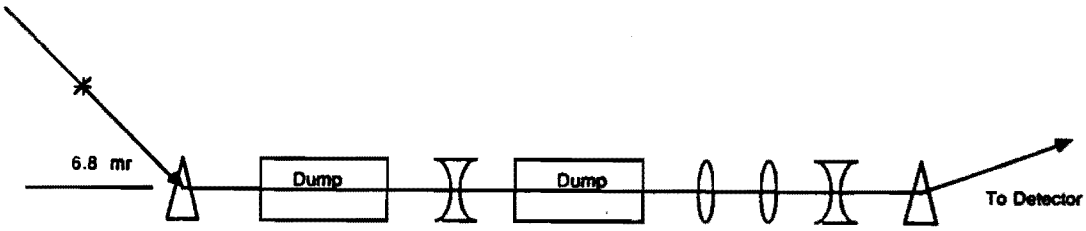

Figure 8: Layout of Proposed Sign-Selected Quadrupole Triplet.

E-744/E-770 in three different ways: (1) from the trigger rate, (2) from the normalization on our charged-current sample, and (3) from the normalization of our neutral current sample (with 1 meter radius and 20 GeV E_H cuts). All three methods indicate that the program predicts the correct number of events to within 20% for the QT beam; we are therefore confident that these statistical estimates are accurate to that precision.

The SQT has a lower flux than the QT beam, but the large bends make the K_L and wrong-sign backgrounds negligible for this beam. The following series of Figures illustrate the nature of the SQT. All plots give the number of interactions for exposures of 10^{18} *pot* within a 1.27 meter radius.

Fig. 9 shows the rates for ν, $\bar{\nu}$, and total ν_e from K_L rates for the Quadrupole Triplet of E-744/E-770. Fig. 10 shows the relative loss (for ν_μ running from the QT; a similar loss occurs for $\bar{\nu}_\mu$.

The wrong-sign background will be discussed further in its own section; the overall level

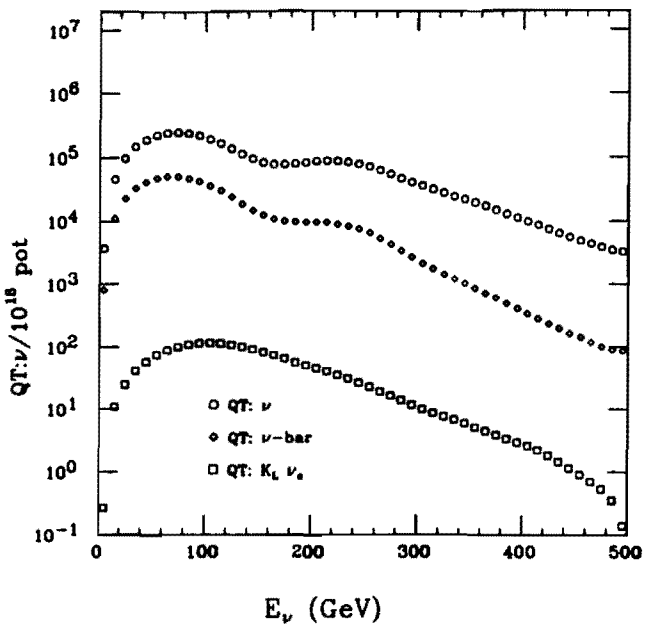

Figure 9: Quadrupole Triplet Fluxes for E-744/E-770.

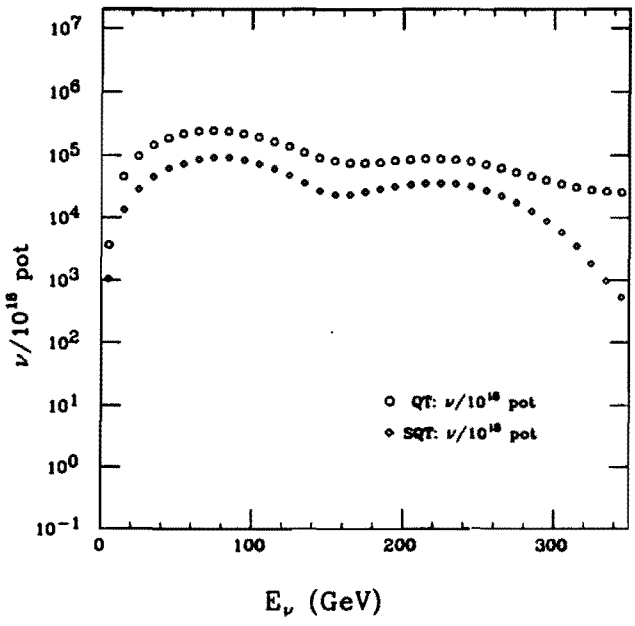

Figure 10: Sign-Selected Quadrupole Triplet Fluxes

is under 0.1%, making the beam more than clean enough to allow separate measurements of ρ and $\sin^2\theta_W$. Furthermore, the remaining samples have mean energies of $\approx$ 30 GeV, and hence can be cut from the data.

Fig. 11 shows the distribution of the remaining ν_e events from $K^{\pm}$ and K_L decay for neutrino data (once again, the antineutrino plot is similar). We see the overall level of K_L is down by a factor of five and once again, the spectrum is soft ($< E_\nu >= 28$ GeV) and can be cut if necessary.

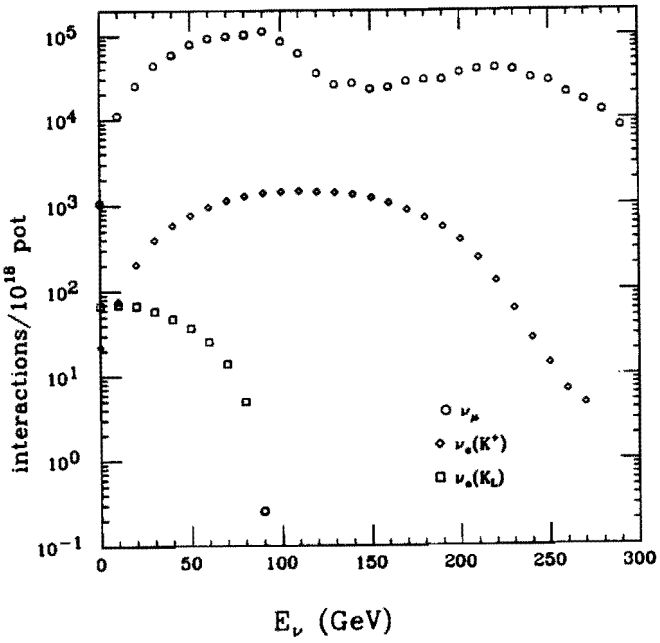

Figure 11: ν_e Backgrounds in the Sign-Selected Quadrupole Triplet.

4 Experimental Systematic Errors in the Determination of $\sin^2\theta_W$ and ρ

There are two major sources of systematic errors in the determination of $\sin^2\theta_W$ and ρ from R_ν and $R_\mathcal{D}$. The first is the presence of ν_e in the beam and the second is the misidentification of charged current events as neutral current. We discuss each in turn.

4.1 ν_e Contamination

The presence of electron neutrinos in the data sample directly affects R_ν since each ν_e event is classified as a neutral current. ν_e's are produced by the decays of kaons: $K^+ \to \pi^o e^+ \nu_e$ and $K_L \to \pi^- e^+ \nu_e$ (and the charge-conjugate states). Other sources (*e.g.*, μ decay) produce negligible contributions for our beam and detector.

Why are the ν_e a source of systematic error? A charged current ν_e interaction

$$\nu_e + N \;\to\; eX \tag{4.1.1}$$

produces an electron which is then lost in the hadronic shower as observed in our detector. Hence every ν_e interaction appears to be a neutral current and therefore their presence biases the observed R_ν. We can compute the magnitude of the effect as follows: assume that the ratio of electron- to muon-neutrino induced events is $\nu_e/\nu_\mu = \beta$. Then

$$\nu_e(NC) + \nu_e(CC) = \beta(\nu_\mu(NC) + \nu_\mu(CC)) \tag{4.1.2}$$

where $\nu_e(NC)$ denotes the number of observed neutral current events from ν_e. Since the definition of R_ν tells us $\nu_\mu(NC) = R_\nu \nu_\mu(CC)$ and all ν_e are observed as neutral currents,

$$\nu_e(NC, obs) \;=\; \beta\nu_\mu(NC)(1 + \frac{1}{R_\nu}) \tag{4.1.3}$$

$$\nu_e(NC, obs)/\nu_\mu(NC) \;\approx\; 4\beta \tag{4.1.4}$$

so the effect on R_ν (or $R_{\bar{\nu}}$) is approximately *four times* as large as the contamination itself.

Our current best estimate of the ν_e contamination in the E-744/E-770/E-733 Quadrupole Triplet Data is 2.5% (which depends on radial and energy cuts). An error of 10% in this value translates to ± 0.005 in $\sin^2\theta_W$, more than twice the desired error, so it is clear that the ν_e contamination must be determined to a few percent of itself.

The presence of K_L in the beam contributes a unacceptably large error. Approximately 1/3 of ν_e interactions arise from $K_L \rightarrow \pi e \nu_e$ and there is no easy way to determine their rate or spectrum. The decay $K_L \rightarrow \pi \mu \nu_\mu$ is responsible for only a few percent of the ν_μ spectrum and is thus difficult to isolate to the required accuracy. Furthermore, there are no data for K_L production applicable to our experiment. The Atherton data[12] normally used at Fermilab were based on 400 GeV data taken at CERN. An extrapolation to 800 GeV produces significant disagreement with the observed ν_μ spectrum so the data are unusable for precision studies. Measurements from E-731 are useful but are sensitive to K_L of energies below 250 GeV, which is too low for our sample, and, furthermore, disagree with Atherton by factors of almost two.[13] It therefore seems prudent to assign a 50% error to the K_L contribution extrapolated from the Atherton parameterization. This leads to an error in $\sin^2\theta_W$ of ± 0.006 which may well be the limiting error of E-744/E-770. Hence if we are to predict the ν_e flux from the measured ν_μ flux we must eliminate the K_L contribution. This is accomplished by the sign-selected quadrupole triplet beam, discussed earlier.

Once we have eliminated the K_L contribution, we need only determine the level of ν_e's from $K^\pm$. There are several potential avenues for measuring this contribution to the required accuracy which have different sources of systematic error. We expect these different methods will complement each other and lead to a small and well-estimated error.

4.1.1 Extraction from the Charged Current Spectrum

The first method uses the observed ν_μ-induced charged current events to provide a measurement of the contaminant ν_e. We estimate the number of $K^\pm$ from the data, and then using the three-body kinematics responsible for ν_e production, generate the spectrum of ν_e at the detector.

The energy-radius correlation of the data permits the π/K separation. The mass difference of pions and kaons induces a distinct energy-radius correlation for the neutrino interaction in the apparatus similar to that of a dichromatic beam. Fig. 12 illustrates the observed QT ν_μ charged current energy spectra in six radial bins. The separation of π and K-induced events is quite clear. The correction from cross-contamination is estimated to be $\approx 10\%$ in this QT data. The overlap comes from two sources: the distributions of two-body decays for π's and K's and the three-body contributions from $K_L, K^\pm \rightarrow \pi\mu\nu$. In the SQT, this contribution will be smaller than 10% since there will be no contribution from K_L. The exact amount is difficult to estimate given the uncertainty in K_L production.

In order to estimate systematic errors, we start with these histograms and then correct for geometrical and kinematic effects. These corrections are typically 10% or less for radii$<$ 1 meter. (There are inbuilt checks, such as the longitudinal vertex distribution, azimuthal rotation of the events to check acceptance, *etc.*, to verify the corrections.) We can then *measure* the $\pi^\pm/K^\pm$ fraction in each radial bin. Fig. 13 shows the π/K contamination for the QT data as a function of radius. Once the relative number of ν_μ induced by $K^\pm$ is known, we can estimate the number and spectrum of ν_e-induced interactions in our apparatus. With the proposed statistical sample of 600K charged current events (after cuts), the statistical error in the estimated ν_e contamination is expected to be less than $< 1\%$ and the corresponding systematic error will be $< 2\%$.

A second and semi-independent method also takes advantage of the charged current data to determine the flux of charged kaons. We can model the particle production of π's and

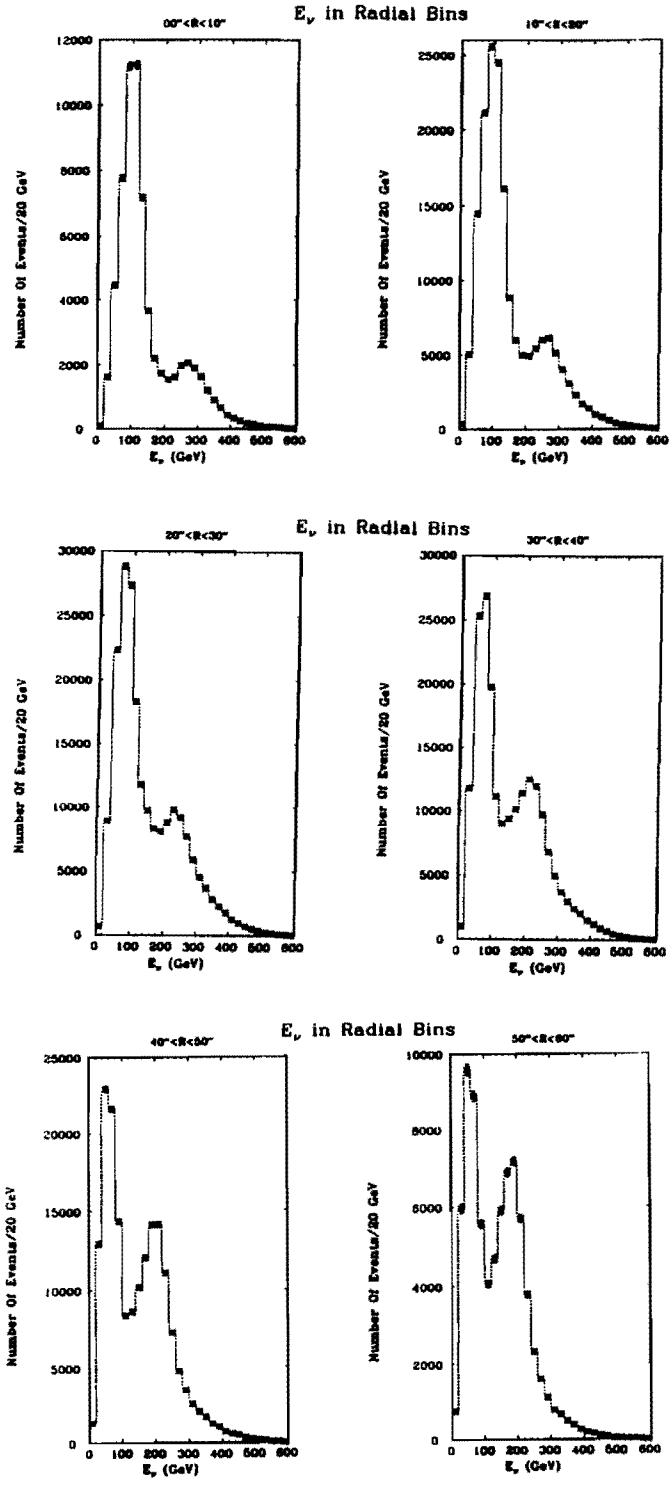

Figure 12: Energy Spectrum in Six Radial Bins for the QT Beam.

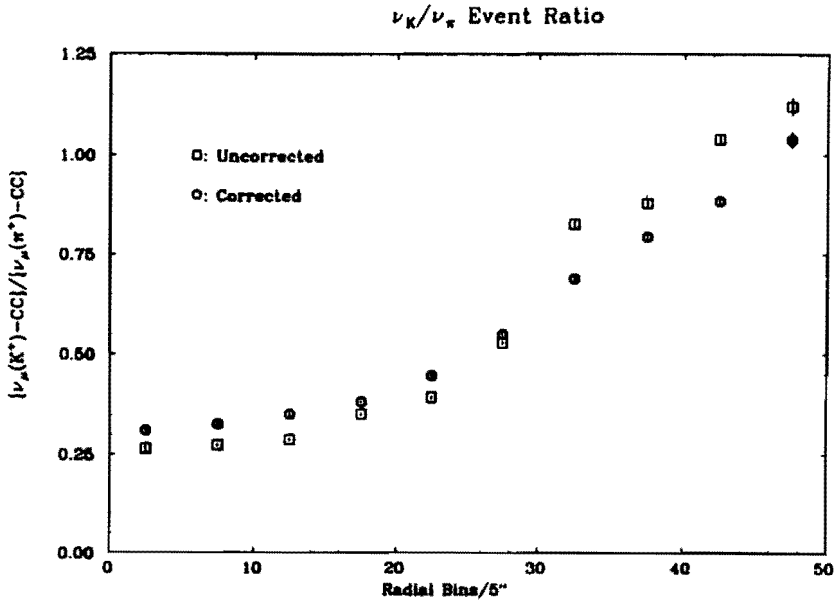

Figure 13: π/K Contamination in the QT.

K's and pass them through the QT train. Next we simulate the decays $\pi^{\pm} \rightarrow \mu\nu$ and $K^{\pm} \rightarrow \mu\nu_{\mu}$ and obtain a fit to the charged-current spectrum. We then have the momentum and angular distributions of parent $K^{\pm}$ produced at the target and can simply change over to the decay mode $K^{\pm} \rightarrow \pi^{o}e\nu_{e}$. A preliminary version of such a modeling of the charged current spectrum of E-744/E770 is shown below using the results obtained from the original 400 GeV Atherton parameterization. We see reasonable agreement for the K^{+}-induced ν_{μ} spectrum but the modeling is far from perfect. We refit the data with the same parameterization as Atherton but let the constants float and obtained the second fit, which is clearly superior. Both plots show data with a 20 GeV E_H cut and a 1.25 meter radius cut.

We can now calculate the ν_e background with either parameterization and extract $\sin^2\theta_W$ with either level of ν_e. The difference in $\sin^2\theta_W$ was only 0.001. The reason for the small shift was that the π/K ratio did not change significantly (and hence the fraction of ν_e within the cuts stayed the same); instead, the spectra shifted slightly. We will continue this line of analysis to understand the fits and procedure better. At this point, it seems reasonable to

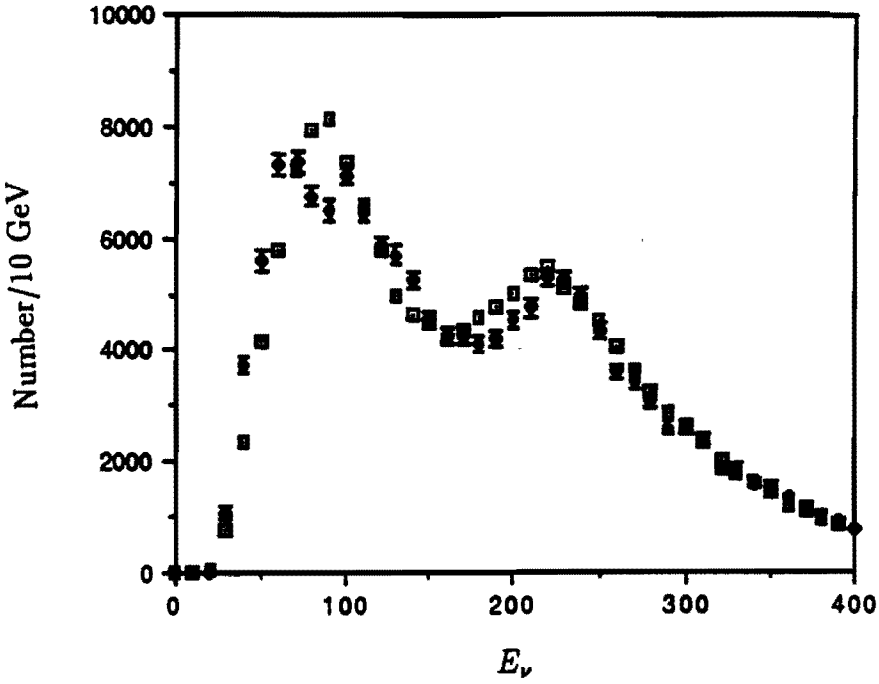

Figure 14: Comparison of Charged-Current Data to Atherton Prediction. The boxes show the data; the points with errors are the result of the MC simulation discussed in the text.

state that the variation in $\sin^2\theta_W$ in the SQT from the remaining $K^\pm$ will be ± 0.001. This is an overestimate since the Atherton model is obviously inadequate and is outside the errors. At a later date we will use the errors from the fit itself to assign errors to ν_e production.

4.1.2 Extraction from Shower Shape

We may use a direct method as well and attempt to identify low-y ν_e interactions in the detector in which most of the ν_e's energy went into the electron. Here we use the fact that electromagnetic showers are shorter than hadronic showers. We define a quantity η_3 such that the ratio of total calorimetric energy to that in the first three counters $= 1 - \eta_3$. For events with energies < 50 GeV, we might use an analogous two-counter variable η_2. Events with η_3 near zero have nearly all their energy in the first few counters and are thus likely to be electromagnetic in origin; events with η_3 near unity are spread out along many consecutive counters, and thus are likely to arise from hadronic showers. Fig. 16

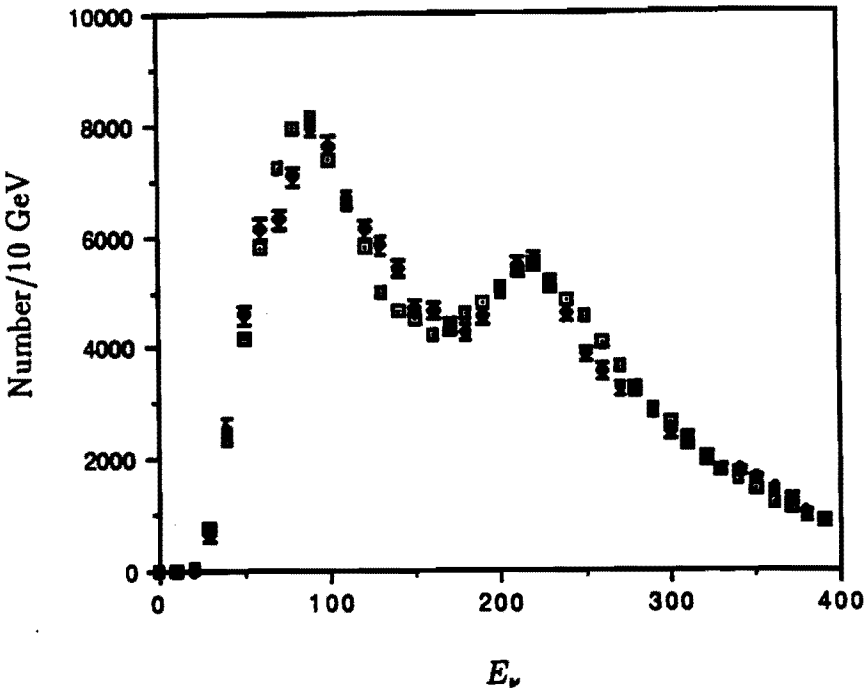

Figure 15: Comparison of Charged-Current Data to Fit. The boxes show the data; the points with errors are the same simulation as above with the parameters of the Atherton fit allowed to float from the 400 GeV values.

below shows the η_3 distribution for charged current events in our detector along with a distribution for electromagnetic showers generated by GEANT; we see the expected peaking for electromagnetic showers from ν_e interactions. This distribution must now be folded with the y-distribution of electrons in charged current events and the distribution of shower lengths for the hadronic component. Figure 17 shows the *observed* η_3 distributions for charged and neutral current events, normalized to the sample for $\eta_3 > 0.4$. The curves clearly diverge at small η_3 with a greater fraction for neutral current events, which we interpret to arise from electromagnetic showers from ν_e interactions. Our goal is to model and understand this observed difference from more detailed simulations and test runs of our own, and extract a ν_e spectrum and rate. This analysis is just underway in E-744/E-770.

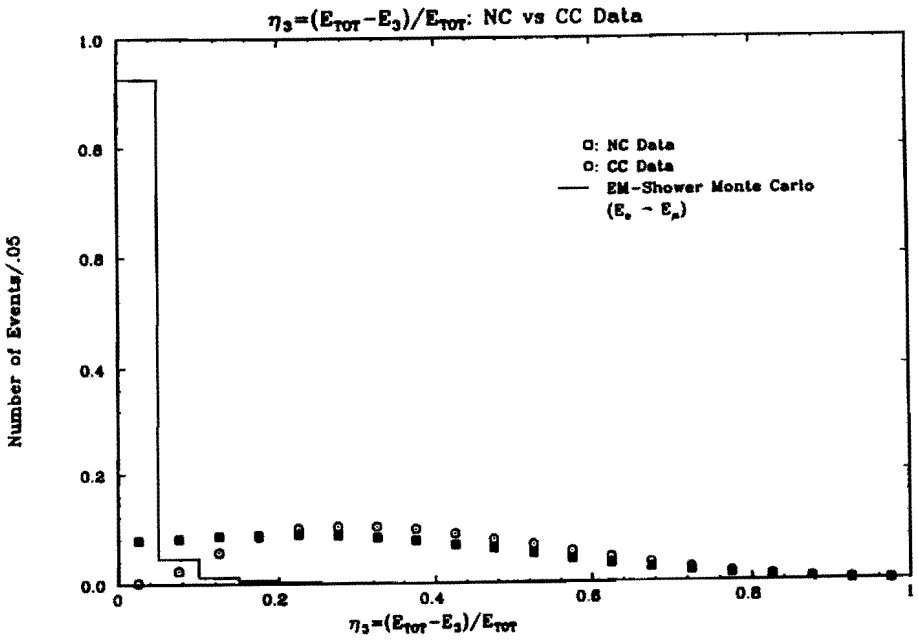

Figure 16: η_3 distribution for Electromagnetic, Charged Current, and Neutral Current showers from GEANT.

As a final note, we mention that the choice of radial cuts plays a strong role in the size of the ν_e subtraction. The kinematics of π and K decay cause ν's from parent K's to preferentially occupy the outside of the detector (the well-known energy-radius correlation), as was shown in Fig. 13. It is clear we can reduce the ν_e contamination significantly by

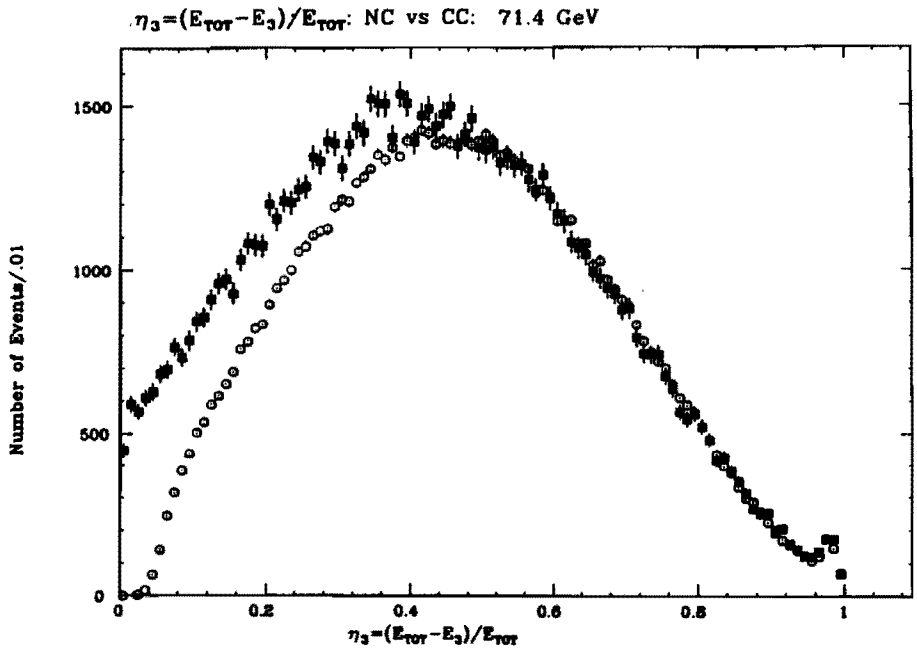

Figure 17: η_3 Distribution for Charged and Neutral Current Events as Measured in E-744/E-770.

reducing the fraction of ν_K. However, we pay for this with reduced statistics, and, since the remaining π-induced data is at lower energy, a greater sensitivity to slow-rescaling issues. The numbers quoted in this Section have used a 1 meter radius cut, consistent with our choices in the past.

4.2 Charged-to-Neutral Current Crosstalk

This was the primary experimental error in previous determinations and has generated considerable controversy.[14] We have learned a great deal from the E-744/E-770 and E-733 analyses and although it will be the single largest experimental error, we expect it will be manageable. Given its importance, we discuss in detail the source of the error and the state of our analysis. We also describe our Phase I plans for reducing the error and indicate the tests we will make for the Phase II measurement.

The reason for the error is clear: since R_ν, $R_{\bar{\nu}}$, and R^- are ratios of neutral to charged current cross sections, misidentification of charged current events as neutral currents directly biases the ratio. The majority of the misidentified charged current events come from interactions at high-y; therefore the contamination for the ρ measurement from $R_{\bar{\nu}}$ will be smaller than the error on $\sin^2\theta_W$ from R_ν since the y-distribution of $\bar{\nu}q$ interactions follows $(1-y)^2$ rather than the approximately flat-y distribution of νq scattering. We therefore concentrate on the effect of charged current contamination on the measurement of R_ν.

The method used in the past by the CCFR (E-616/701) and CDHS collaborations used the length of the event as determined by scintillation counters to separate charged from neutral currents.[1] Charged current events produce a muon, which fires many consecutive scintillators, whereas a neutral current event lasts only as long as does the hadronic shower (typically 1–2 meters of Fe). Charged current events with short lengths come from two nearly equal sources: (1) low energy (high-y) muons which range out inside the shower, and (2) wide-angle muons which exit the calorimeter before they have traversed enough counters to be recognized (which tend to be at large-x).[2] Note that the length–method does not attempt to track these wide angle muons; nor does it use any information on the transverse position of minimum-ionizing particles as determined by calorimetry. We will improve the error on the contamination by using tracking and will explore the use of an improved calorimeter.

The analyses of CCFR and CDHS, while quite different in details, both had subtractions of order 20% because of their similar target densities (both used iron) and energy range. Each experiment achieved an error of ± 0.002 on $\sin^2\theta_W$ from the charged current subtraction; although the CCFR experiment had to impose a y cut due to their inability to either detect or model correctly wide angle muons. The next generation CCFR experiment (E-744/E-770) has achieved a somewhat smaller error without the y cut. P–815 will further reduce

[1] In the E733 fine-grained calorimeter, NC and CC data were separated on an event-by-event basis by identifying penetrating tracks. This is ultimately a better method but requires a different calorimeter from Lab E.

[2] Since $\theta_\mu^2 = 2m_N x(E_\nu - E_\mu)/E_\nu E_\mu$).

the error.

How will we lessen the contaminations? First, the higher-energy Quadrupole Triplet runs of E-744/E-770 reduced this subtraction to 14%. The beam proposed for this experiment will have a lower mean energy (127 GeV compared to 143 GeV for E744/E770) raising the level to 16%, but still below the 20% of the old experiments.

Simulations show that half of the charged current subtraction comes from muons which exit the side of the calorimeter, and half from muons which range-out within the hadronic shower. If we can identify these exiting muons, then the subtraction will decrease acccordingly. As mentioned earlier, this identification removes events at large-x; their contribution is the most uncertain because the structure functions at high-x are the least well determined. After the wide angle events are removed, the remaining high-y sample will have a smaller proportional error. In addition, the structure functions at high-x are now much better determined (after E-744/E-770) and there will be a significant decrease from that improvement as well, even if tracking is not utilized.

We can recognize exiting muons in two ways: either through software (tracking muons in our drift chambers) or through hardware (a scintillator-based veto system). Using the existing apparatus is easier and less expensive than building new equipment, but the tracking algorithms are still at an early stage of development. We have decided for this proposal to concentrate on developing our tracking algorithms to better identify wide angle muons. In addition, we will explore the possibility of a scintillation-based veto system in the Phase II prototype.

We have already begun to improve our algorithms for tracking muons within the target. The old CCFR analysis could not pursue this method with its spark chambers, but the FNAL-constructed drift chambers used in E-744/E-770 are far better devices and we are actively developing tracking code for wide-angle muons. Preliminary studies tell us that we can track approximately 90% of exiting muons at short length; the error on this method will

then come from errors on the tracking efficiency.

We are studying the use of transverse information from the calorimeter which will greatly reduce the subtraction. We may wish to replace each of the liquid scintillation planes with a plastic scintillation hodoscope; there will be alternating x and y staves where the old $10' \times 10'$ liquid scintillators currently exist. The inner staves can be several feet across, but surrounding them will be outer staves that are appromimately six inches across. The final sizes will be determined from Monte Carlo simulations and cost considerations. These counters will serve to tag exiting minimum ionizing particles. If we place the same software cut on charged and neutral currents, we will reduce the subtraction a factor of two with negligible systematic error. If we decide for Phase II that sampling the shower twice as often is desirable, then these new counters would be built at that time.

Given the controversy between the error analyses of CDHS and CCFR, E-744/E-770 has repeated the charged current subtraction using the event length subtraction method of both experiments on its data sample. The CDHS method used an energy-dependent length for the shower; if the shower was shorter than the cut, it was classified as a neutral current. They then normalized the subtraction of short-length events with events at lengths of about twice the cutoff(effectively normalizing the high-y background with events at intermediate y). The CCFR analysis cut at a fixed length of 210 cm of Fe. This analysis employed a y-cut using the radius-energy correlation. As a check, CCFR used two different normalizations, one from the intermediate length events (as did CDHS) and another from all events with lengths greater than the cut. Figs. 18 and 19 below shows the neutral current data and a Monte Carlo simulation of the charged current background in the high-energy E-770 sample. The fixed and scaled-length methods (for the scaled–length method, $l/l_o = 1$ implies 98% of all showers are contained within that length) are shown. We have normalized the subtraction in two ways as did the old CCFR analysis, since this was a good test of potential systematic error. The disagreement and total systematic error by both methods (fixed and scaled length) and both normalizations (all events and intermediate length) is only ± 0.0025 or 1% of $\sin^2\theta_W$.

Hence, the fractional error on R_ν due to *normalization uncertainty* of the short charged current background is 0.46%. We believe that by effectively using tracking, we can decrease this normalization error by a factor of approximately $\sqrt{2}$, leaving a total error of 0.35% on R_ν.

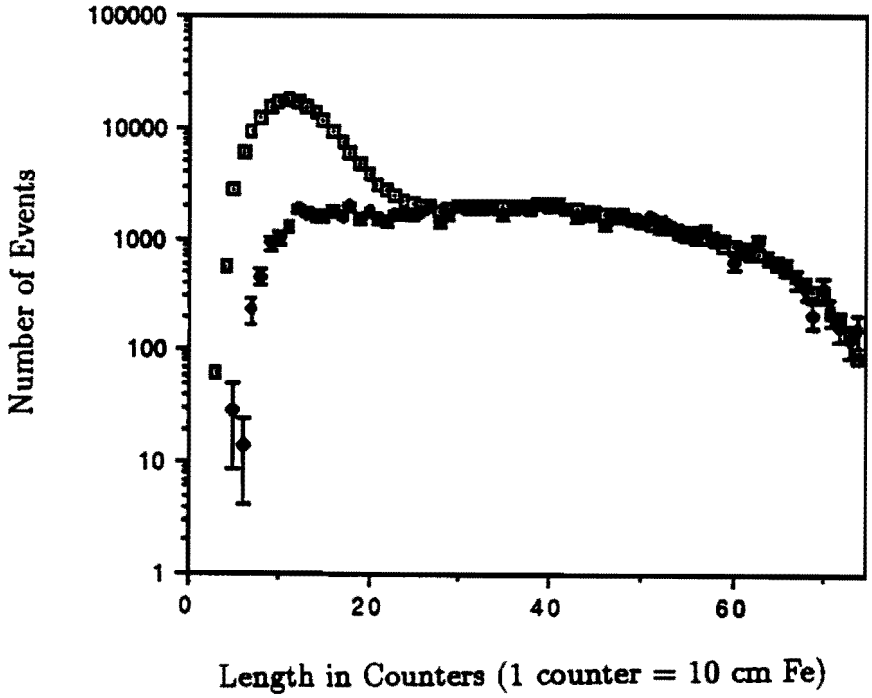

Figure 18: Fixed–Length Distribution of E-744/E-770 Data and Monte Carlo Simulation. The boxes show the data with the NC peak at small lengths; the overlay is the CC simulation.

The choice of radial cut plays an important role here as well as in the discussion of ν_e contamination. As we cut away from the edge of the detector, it is progressively less likely that a muon will be missed (until we reach a plateau from those muons which range out within the shower). The numbers quoted here are for a 1 meter radial cut; Fig. 20 shows the fraction of neutral current contamination as a function of radius cut in the E-744/E-770 data. A detailed study of the tradeoffs between charged current contamination, ν_e background, statistics, and slow-rescaling effects will give the final set of cuts, and, perhaps more importantly, studying the data as a function of these cuts will also help us understand the systematic errors. Our choice of 1 meter is based on early E-744/E-770 analysis and can certainly change depending on future work.

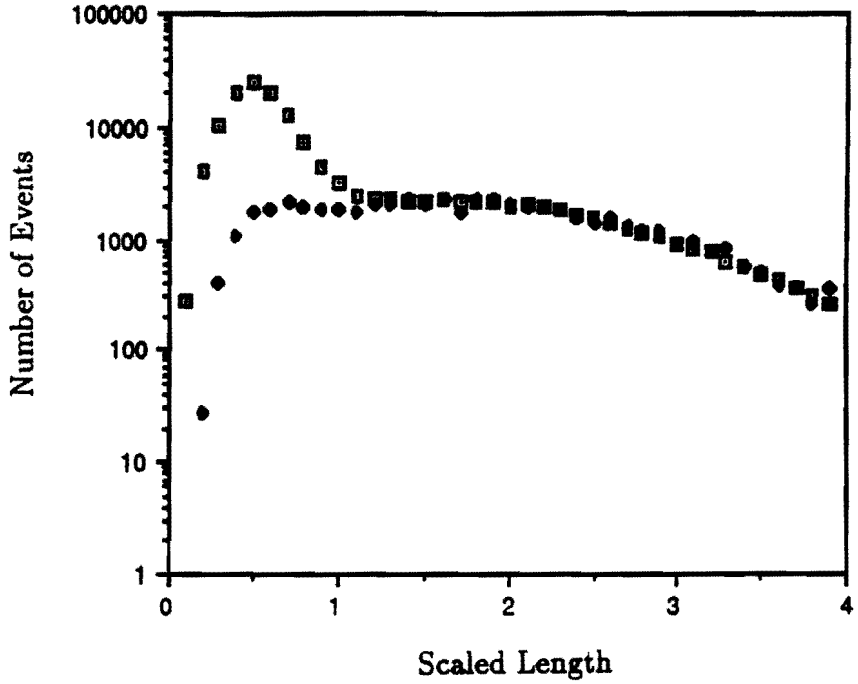

Figure 19: Scaled–Length Distribution of E-744/E-770 Data and Monte Carlo Simulation. The boxes show the data in 1 counter bins with the NC peak at small lengths; the overlay is the CC simulation.

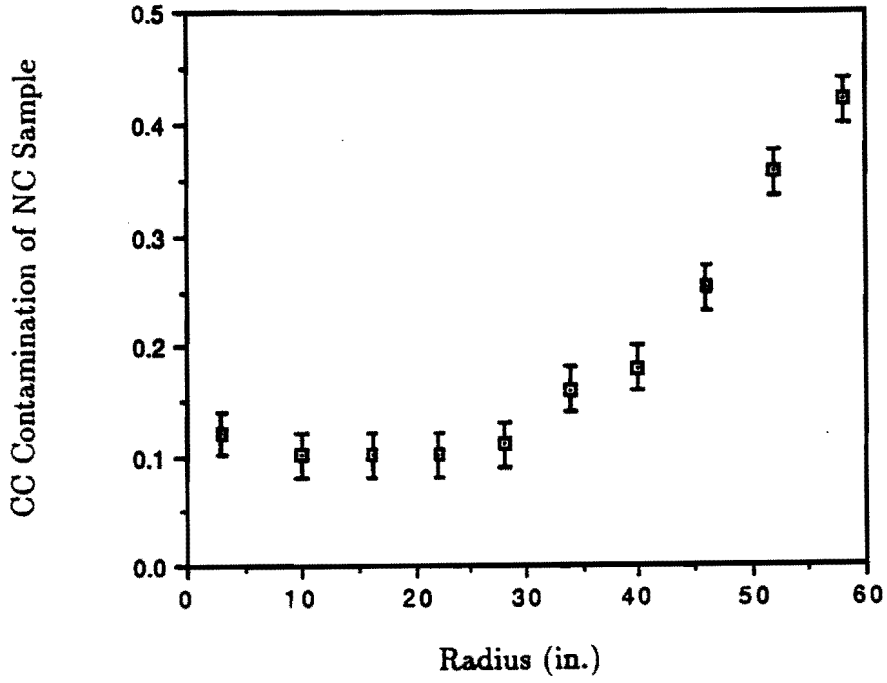

Figure 20: Fraction of Neutral Current Sample from Misidentified Charged Current Data.

In addition to the normalization error on the charged current subtraction, there will be an uncertainty due to the shape of the short CC event length distribution. Part of this latter effect arises from uncertainties in the x and y distributions of charged current events; but the dominant contribution is from a possible systematic misdetermination of the event length. By comparing the agreement of the E744/E770 data to our Monte Carlo, we estimate that the systematic error on the length determination of a shower is approximately 1.7 cm of steel. This translates into an additional fractional error on R_ν of 0.3% . When added to the normalization error, the total error on R_ν from the charged current subtraction is estimated as 0.46%.

Our conclusion is that by employing the transverse information from improvements in the tracking analysis, and better knowledge of structure functions, the error from charged current crosstalk will be approximately 1% on $\sin^2\theta_W$ and one-half that amount on ρ^2 (1/4% of ρ).

4.3 Relative $\nu/\overline{\nu}$ Flux Uncertainties

The relative neutrino/antineutrino flux, $f = \phi^\nu/\phi^{\overline{\nu}}$, and relative spectrum are needed to calculate $\sin^2\theta_W$ and ρ in both the LS and P-W methods. For the LS method, the relative flux enters in calculating r. In the P-W method, the relative flux is needed to calculate R^+ and R^-; since these quantities depend on sums and differences of cross-sections, the P-W method is more sensitive to the relative fluxes and spectra than is the LS technique.

The principal method of relative flux extraction is derived from the most general form of the $(V-A)$ ν-N cross section:

$$\frac{d^2\sigma^{\nu,\overline{\nu}}}{dxdy} = \frac{G_F^2 ME}{\pi}\left((1-y-\frac{Mxy}{2E})F_2 + \frac{y^2}{2}2xF_1 \pm (y-\frac{y^2}{2}xF_3)\right)$$

In the limit $y \rightarrow 0$ or $\nu = E_{had} \rightarrow 0$, the differential cross section $d\sigma/d\nu$ approaches a

constant which is independent of energy and is the same for neutrinos and antineutrinos.[15] When integrated over all x and values of ν up to a cutoff value, ν_0, the cross section becomes independent of energy. The relative flux is then determined by the cross section below ν_0 measured from the number of events with $\nu < \nu_0$:

$$\phi(E) \propto N(E, \nu < \nu_0) + \mathcal{O}(\nu_0/E)$$

where $\mathcal{O}(\nu_0/E)$ indicates corrections of order ν_0/E arising from helicity induced y-dependent terms (of order 5–10%). The cutoff, ν_0, is chosen small enough to minimize these corrections, but large enough to provide sufficient statistics. With this method, the relative flux in E744/E770 has been determined to $\delta f/f = 1.5\%$ which will be used in estimating the P815 relative flux errors. Two other techniques have also been used in the E744/E770 analysis to verify the relative flux extraction: the extrapolation of the y-distributions to $y = 0$ and the comparison of the structure functions at fixed x and Q^2 for varying neutrino energy bins. These alternative techniques agree with the fixed ν method at the level of 1.5 to 2%.

For the LS method, the cross section ratio is calculated by taking the ratio of observed events corrected for spectrum and efficiency differences.

$$\frac{\sigma_{\bar{\nu}}^{CC}}{\sigma_{\nu}^{CC}} = \left(\frac{N_{\bar{\nu}}^{CC}}{N_{\nu}^{CC}}\right)\left(\frac{\epsilon_{\nu}}{\epsilon_{\bar{\nu}}}\right) f$$

Since the efficiency correction is well understood, we estimate that the systematic error in r will be dominated by the relative flux error of 1.5%. Referring to Eq. 2.1.3 we note that:

$$\frac{dR_{\nu}}{dr} = \rho^2\left(\frac{5}{9}\sin^4\theta_W\right) \approx 0.029 \qquad (4.3.5)$$

and

$$\frac{dR_{\bar{\nu}}}{dr} = -\rho^2\left(\frac{5}{9}\sin^4\theta_W\frac{1}{r^2}\right) \approx -0.164 \qquad (4.3.6)$$

for $r = 0.423$ and $\sin^2\theta_W = 0.230$ as would be expected with a 10 GeV hadronic energy cut. The flux error then contributes an error of $\pm 0.06\%(\pm 0.34\%)$ for R_{ν} and $R_{\bar{\nu}}$ respectively and introduces a negligible contribution to the $\sin^2\theta_W$ error.

For the P-W method, the relative flux is needed to form the cross section ratios, R^+ and R^-, from the measured number of events.

$$R^{\pm} = \left(\frac{N^{\nu}_{NC} \pm f N^{\bar{\nu}}_{NC}}{N^{\nu}_{CC} \pm f N^{\bar{\nu}}_{CC}} \right)$$

An error in the relative flux introduces an error in $R^{\pm}$ of:

$$\frac{dR^{\pm}}{df} = \frac{N^{\bar{\nu}}_{NC} - R^{\pm} N^{\bar{\nu}}_{C} C}{N^{\nu}_{CC} \pm f N^{\bar{\nu}}_{CC}}$$

For $\delta f/f = \pm 1.5\%$, $f = 2.9$, $R^+ = .338$, and $R^- = .269$, the above derivatives are .0047 and .0318 and the derived fractional errors on $R^{\pm}$ are .06% and .53% for R^+ and R^- respectively.

4.4 Other Experimental Corrections

Several small experimental corrections must be made in addition to the charged current and ν_e subtractions. The most important of these are due to cosmic ray backgrounds and wide band neutrino backgrounds, and to neutral current events with long event lengths that are misclassified as charged current events.

In the CDHS experiment, the cosmic ray background subtraction produced a correction on R_ν of $-2.0 \pm 0.1\%$. The correction is negative because cosmic ray events typically consist of soft shower particles entering the detector vertically which produce a short event length. There is no need to improve the accuracy of this subtraction for a new precision measurement of R_ν. However, we can decrease the uncertainty on the cosmic ray subtraction by at least a factor of ten by taking more triggers between spills, and thus reducing the statistical error on the subtraction; and by employing drift chamber hit information to reject events in which a shower of soft particles or a single unaccompanied muon is seen entering the side

of the detector. For $R_{\bar{\nu}}$, the subtraction is larger since the cosmic rate is constant while the antineutrino cross section folded with the antineutrino flux is about five times less than for neutrinos. Again, however, the already adequate precision on this subtraction obtained by CDHS can be reduced by a factor of four by taking more cosmic triggers. The error in the P-W variables is of comparable size with R^- suffering somewhat from its dependence on a difference of cross-sections. In summary then, the error due to cosmic ray subtraction will be less than or equal to 0.01%, 0.05%, and $<<$ 0.12% for R_ν, $R_{\bar{\nu}}$, and R^-, respectively.

The CDHS subtraction for wide band neutrinos—neutrinos produced by any other mechanism than from pion or kaon decay in the decay region— was $-1.2 \pm 0.1\%$. This background was important for CDHS to understand since they used beam monitors to measure the flux in the ν and $\bar{\nu}$ beam. Since wide band ν and $\bar{\nu}$ do not originate from the pions and kaons in the dichromatic beam, the flux measurements were not sensitive to this contribution. The CCFR experiment, in contrast, uses the neutrino data itself to determine the flux. The wide band background just adds to the dominant signal producing no effect on R_ν, $R_{\bar{\nu}}$, or R_{PW} to first order. The WBB background affects R_ν only through the presence of $\bar{\nu}$ in the ν beam. This effect will be quite small in the proposed beam. Only $0.010 \pm 0.001\%$ of all charged current events in the ν beam are expected to be initiated by wide band $\bar{\nu}$ neutrinos. The corresponding number for the $\bar{\nu}$ beam is $0.12 \pm 0.03\%$ contamination by ν induced interactions. The only possibility of the wide band background becoming important is if the ratio of ν_e to ν_μ events in the wide band portion of the flux is substantially larger than the corresponding ratio for the SST beam, a possibility that seems highly unlikely since the primary proton beam points more than 7.0 mrad away from the Lab E detector (after both dipoles). We conclude that the effect of a wide band background will be totally negligible.

The long shower correction on R_ν was $+0.5 \pm 0.2\%$ at CDHS. This error is adequate for a new precision experiment. The CCFR detector will have roughly the same magnitude for the correction since it is an iron calorimeter like CDHS. The correction is also at least as well understood as in CDHS due to extensive test beam runs in the past. With more test

beam data, it should be feasible to reduce the error on this correction by a factor of at least two.

5 Theoretical Uncertainties Associated with the $\sin^2\theta_W$ Extraction

5.1 Charm Mass and Strange Sea Uncertainties

In the extraction of $\sin^2\theta_W$ in deep-inelastic neutrino-nucleon scattering using the Llewellyn Smith formulation the largest theoretical uncertainty is the charm quark mass correction. Since charged current interactions can produce a charm quark from a down or strange quark, this component of the cross section affects only the denominator of R_ν, $R_{\overline{\nu}}$, and R^+. On the other hand, the determination of $\sin^2\theta_W$ using the P-W variable, R^-, is insensitive to the charm quark mass since it is defined by the difference in ν and $\overline{\nu}$ cross sections leading to a substantial cancellation of the charm production terms.

The relative magnitude of the charm quark contribution to the charged current cross section depends on the mass of the charm quark, m_c, through the slow rescaling variable $\xi = x + m_c^2/2MyE_\nu$ and the helicity factor $(1 - m_c^2/2ME_\nu\xi)$. Imprecise knowledge of m_c leads to an error in the correction of this effect. Recent data on neutrino-nucleon dimuon production has shown that the slow rescaling prescription is a good representation of the threshold energy dependence of this process. The charm mass parameter has been measured to be $m_c = 1.34 \pm 0.33$ GeV[16]. Over the next year, the analyzed statistics will be increased by a factor of two from the combination of E744 and E770. This will reduce the charm mass error to $\delta m_c = \pm 0.25$ GeV.

An additional source of error in the correction of the charm quark contribution comes from the errors in the quantity of the strange sea, quantified by the parameter $\kappa = 2S/(\bar{U} + \bar{D})$. The present average value of this parameter is $\kappa = 0.492 \pm 0.054(\text{stat.}) \pm 0.024(\text{syst.})$[16]. The uncertainties in m_c and κ translate into a corresponding uncertainty in $\sin^2\theta_W$ by the values shown in Table 7. In this calculation we have required that the hadron energy satisfy $E_H > 10$ GeV for both neutral and charged current events, where E_H is the recoil hadronic

energy.

Another tack is to correct for the charm quark component of the cross section directly. We note that the charm quark contribution in dimuon production is the same as in deep-inelastic scattering except for the additional terms of the charm quark fragmentation function, $D(z)$, and the semileptonic branching ratio, B_c of the produced mixture of charmed particles. In deep-inelastic scattering:

$$\frac{d^2\sigma^\nu}{dx\,dy} = \frac{d^2\sigma^\nu}{dx\,dy}|_{noncharm} + \frac{G_F^2 M E_\nu}{2\pi}(1-y+\frac{xy}{\xi})[(\xi u+\xi d)|V_{cd}|^2 + 2\xi s|V_{cs}|^2] \qquad (5.1.1)$$

and in dimuon production:

$$\frac{d^2\sigma^\nu_{2\mu}}{dx\,dy\,dz} = \frac{G_F^2 M E_\nu}{2\pi}(1-y+\frac{xy}{\xi})[(\xi u+\xi d)|V_{cd}|^2 + 2\xi s|V_{cs}|^2]D(z)B_c \qquad (5.1.2)$$

The dimuon data therefore allow the charm quark component of the deep-inelastic cross section to be extracted from

$$R_o = R_\nu/(1-\frac{R_{2\mu}}{\epsilon B_c}). \qquad (5.1.3)$$

where $R_{2\mu}$ is the measured ratio, $R_{2\mu} = N_{2\mu}/N_\mu$, and ϵ is the acceptance efficiency which normalizes the dimuon data to the same energy cuts used for the charged current data. The ratio R_o has a significantly reduced sensitivity to the charm mass since most of the charged current charm production has been subtracted. The principal error in this technique arises from the uncertainty in the branching fraction B_c which at the present time is known to roughly $\pm 10\%$ [16]. Future determinations of B_c using all the existing Tevatron dimuon data should reduce this error to $\pm 6\%$.

The errors of this method as well as those of the "conventional" R_ν analysis are given in Table 7. Using R_o to determine $\sin^2\theta_W$ yields about the same error, but has a different set of systematics from the Llewellyn Smith R_ν method and will be useful in checking systematics.

Table 7: The errors in the LS ratio and in the charm-corrected ratio R_o.
It is assumed: $\delta m_c = \pm 0.25$ GeV/c^2, $\delta\epsilon = \pm 0.05$,$\delta\kappa = \pm 0.06$, $\delta B_c = \pm 0.007$, and 4000 dimuon events.

ν_μ	$\delta R_\nu/R_\nu\|_{m_c} = \pm 0.0056$	$\delta R_o/R_o\|_{m_c} = \pm 0.0018$
	$\delta R_\nu/R_\nu\|_{\kappa} = \pm 0.0009$	$\delta R_o/R_o\|_{\kappa} = \pm 0.0014$
		$\delta R_o/R_o\|_{B_c} = \pm 0.0054$
$\bar{\nu}_\mu$	$\delta R_{\bar{\nu}}/R_{\bar{\nu}}\|_{m_c} = \pm 0.012$	$\delta R_o/R_o\|_{m_c} = \pm 0.0018$
	$\delta R_{\bar{\nu}}/R_{\bar{\nu}}\|_{\kappa} = \pm 0.0022$	$\delta R_o/R_o\|_{\kappa} = \pm 0.0078$
		$\delta R_o/R_o\|_{B_c} = \pm 0.0054$
	$\delta \sin^2\theta_W = \pm 0.0028$	$\delta \sin^2\theta_W = \pm 0.0030$

5.2 Nonisoscalar Correction

Certain cancellations which make the Llewellyn Smith formulation insensitive to higher twist effects depend on the neutrino target being isoscalar. Since the Lab E neutrino target is composed of mostly iron, which has a 6.89% excess of neutrons, a correction for the excess of d-valence quarks must be made. Accordingly, the CC cross sections are modified by the following additional terms. For neutrino CC scattering

$$\frac{d^2\sigma}{dx\,dy}|_{I\neq 0} = \frac{d^2\sigma}{dx\,dy}|_{I=0} + A\beta[xu_v - xd_v] \tag{5.2.4}$$

and for antineutrino CC scattering

$$\frac{d^2\sigma}{dx\,dy}|_{I\neq 0} = \frac{d^2\sigma}{dx\,dy}|_{I=0} - A\beta[xu_v - xd_v](1-y)^2 \tag{5.2.5}$$

where $A = {G_F}^2 M E_\nu/\pi$ and $\beta = (N-Z)/(N+Z)$. In the expressions above we have neglected KM matrix terms which are nearly 1 and contribute a small error. The nonisoscalar terms tend to make the neutrino CC cross section larger and the antineutrino cross section smaller. There are corresponding terms which modify the NC cross sections that depend on

the $xu_v(x,Q^2)$ and $xd_v(x,Q^2)$ quark distributions as well as the gauge coupling constants of the standard model δ_i given by Eq. 2.1.1 above. For neutrino NC scattering

$$\frac{d^2\sigma^{NC}}{dx\,dy}|_{I\neq 0} = \frac{d^2\sigma^{NC}}{dx\,dy}|_{I=0} + A\beta[(\delta_2{}^2 + \delta_4{}^2(1-y)^2) - (\delta_1{}^2 + \delta_3{}^2(1-y)^2)](xu_v - xd_v) \quad (5.2.6)$$

and for antineutino NC scattering

$$\frac{d^2\sigma^{NC}}{dx\,dy}|_{I\neq 0} = \frac{d^2\sigma^{NC}}{dx\,dy}|_{I=0} + A\beta[(\delta_2{}^2(1-y)^2 + \delta_4{}^2) - (\delta_1{}^2(1-y)^2 + \delta_3{}^2)](xu_v - xd_v) \quad (5.2.7)$$

Note in Eqs. 5.2.4 and 5.2.5 that the nonisoscalar correction is proportional to the difference $(xu_v - xd_v)$, but in the NC case there are additional multiplicative terms which are proportional to the difference between electroweak coupling terms. For $\sin^2\theta_W \approx 0.230$ these additional NC terms are small making the CC correction the dominant term.

To estimate the magnitude of the nonisoscalar correction we use a parameterization[18] of the E744/E770 structure functions in a simulation of the proposed experiment including the energy spectrum of the incident neutrino beam. The results are given in Table 8 below where the ratio of the cross sections from an iron target are compared to that of an isoscalar target. In the calculation we have taken $\sin^2\theta_W = 0.225$ and assumed an isoscalar sea where $x\bar{u}(x,Q^2) = x\bar{d}(x,Q^2)$. The hadronic energy for the NC and CC events was required to be greater than 10 GeV.

The primary experimental error in this correction originates from the uncertainty in the measured $xu_v$and xd_v distributions. The best measurements of these valence distributions come from deep-inelastic electron- and muon - nucleon scattering. In Fig. 21 we show a comparison of recent data taken on the ratio $F_2(n)/F_2(p)$ as a function of x. Note that the NMC data and the BCDMS data[17]are in good agreement in the overlap region indicating that the systematic errors between these experiments is $< \pm 10\%$. The SLAC data tend to be somewhat higher in the large x region than the CERN experiments but are in a lower Q^2 domain. As a measure of the sensitivity to measurement errors in the valence quark distribution we have computed the NC/CC ratio by allowing the d_v/u_v ratio to change by

Table 8: The ratio of the iron cross sections to their isoscalar counterparts using the structure function parameterization of experiment E744/E770 with $E_H > 10$ GeV.

Cross-Section Comparison	Ratio
νN scattering:	
$\sigma_{CC}(\text{Fe})/\sigma_{CC}(\text{isoscalar})$	1.0178
$\sigma_{NC}(\text{Fe})/\sigma_{NC}(\text{isoscalar})$	1.0030
$R_\nu(\text{Fe})/R_\nu(\text{isoscalar})$	0.9855
$\bar{\nu}N$ scattering:	
$\sigma_{CC}(\text{Fe})/\sigma_{CC}(\text{isoscalar})$	0.9886
$\sigma_{NC}(\text{Fe})/\sigma_{NC}(\text{isoscalar})$	0.9997
$R_{\bar{\nu}}(\text{Fe})/R_{\bar{\nu}}(\text{isoscalar})$	1.0113

$\pm 10\%$. The result is $\delta R_\nu/R_\nu = \pm 0.11\%$ and $\delta R_{\bar{\nu}}/R_{\bar{\nu}} = \pm 0.05\%$. For a one-parameter determination of $\sin^2\theta_W$ these errors translate into $\delta \sin^2\theta_W = \pm 0.0006$ and $\delta\rho = \pm 0.03\%$, where we have simply used $R_{\bar{\nu}}$ to determine ρ. For a two dimensional analysis, taking into account the correlation between the R_ν and $R_{\bar{\nu}}$ errors we find $\delta \sin^2\theta_W = 0.0008$ and $\delta\rho = \pm 0.03\%$. In both cases the resultant uncertainties in $\sin^2\theta_W$ are within our criterion of $\delta \sin^2\theta_W / \sin^2\theta_W = \pm 1\%$.

A check of the isoscalar correction can be made by building a special isoscalar section of the neutrino target. By measuring the ratio of the number of CC events normalized to the same target mass, $N_{CC}(\text{Fe})/N_{CC}(\text{isoscalar}) = \sigma_{CC}(\text{Fe})/\sigma_{CC}(\text{isoscalar})$, we can probe the nonisoscalar term $[xu_v - xd_v]$ directly. For a 10% measurement of the 1.78% isoscalar effect (refer to Table 8) we would need about 320K CC events from the isoscalar section of the neutrino target. A significant beam exposure ($N_{CC}(\nu) > 10^6$) would be needed to reach this level for a practical experiment. This option will be explored in Phase II.

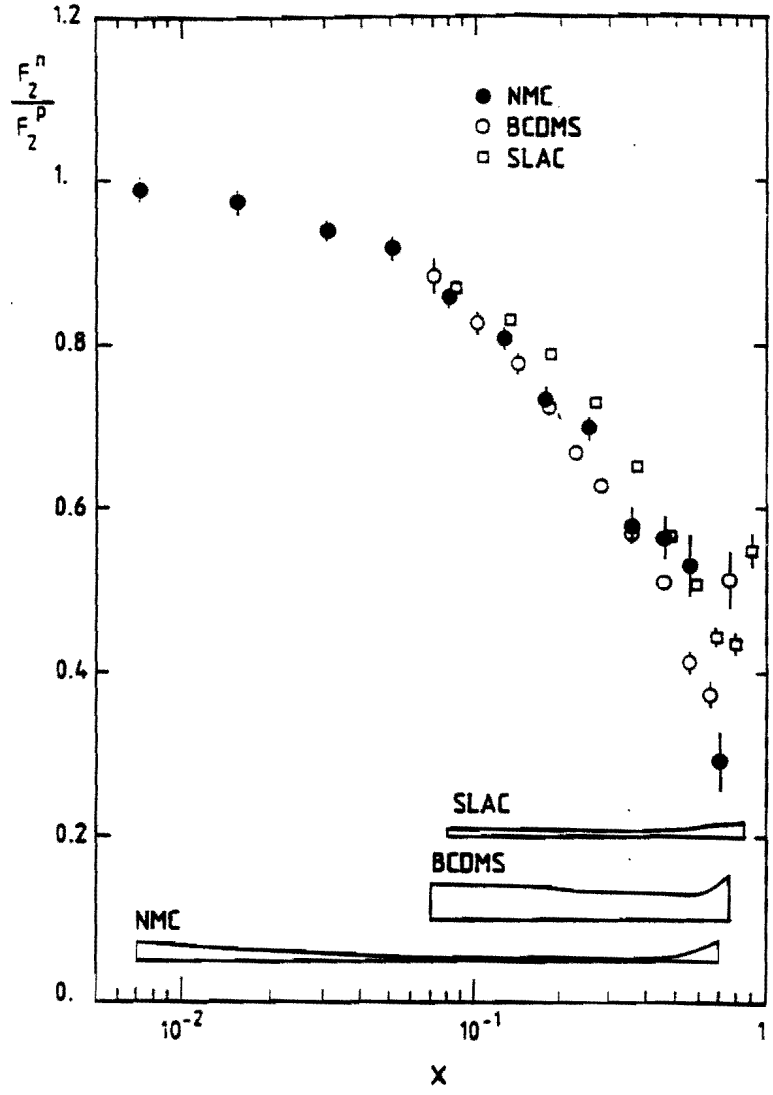

Figure 21: $F_2(n)/F_2(p)$ *vs.* x.

5.3 Electromagnetic Corrections

There is a class of radiative corrections which is due to real or virtual photon emission from the fermions (quark or lepton). While it is somewhat artificial to separate photonic corrections from the body of electroweak phenomema, to one loop order these processes are in principle calculable from purely QED considerations. One contribution to the electromagnetic radiative corrections derives from bremsstrahlung from the muon in the charged-current interactions, a process with no counterpart in the neutral-current interactions. The energy of muon-bremsstrahlung photons tends to add to the experimentally measured E_{had}, and therefore artifically enhances the CC to NC ratio. A larger contribution comes from the γW "box" diagram which is only present for the charged current processes. We estimate the size of the resulting correction to be 1.2% and 2.0% for R_ν and $R_{\overline{\nu}}$ respectively. This correction translates into a correction to $\sin^2\theta_W$ of order -0.006, relatively large compared to the top quark and Higgs boson mass effects.

Fortunately, a large body of progressively more detailed theoretical work[19, 20, 21, 22, 23] during the last 10 years or so has made the reliable calculation of these corrections possible. However, the calculations are made within the context of the quark/parton model, and contact with real experimental quantities can only be made by the influx of empirical information in the form of parton distribution functions or, preferably, experimental structure functions. Also, owing to the existence of experimental cuts (e.g. in the parameter y), logarithmic mass singularities are present which lead to a dependence in the calculations on both the initial and final state quark and lepton masses. In an effort to examine the model dependencies mentioned above, Bardin *et al.* have studied the sensitivity of their calculations to two different parameterizations of the structure functions and to a large range in the poorly known quark masses (1 MeV to 1 GeV).[23] In all cases they find that the uncertainties due to distribution functions and quark masses are small compared to the size of the radiative correction.

The results of Bardin *et al.* notwithstanding, the most recent results from DIS-neutrino

experiments include a conservative estimate of the theoretical uncertainty due to radiative corrections mainly based on the comparison of several different calculations [24],[25],[26]. At present the systematic uncertainty in $\sin^2\theta_W$ quoted by all experiments is $\approx \pm 0.002$. We believe it will be possible to reduce the theoretical uncertainty to below $\pm 10\%$ of the correction itself by using the now well accepted Bardin *et al.* calculations as well as presently available improved structure function data[27]. This translates into an error of ± 0.0006 in $\sin^2\theta_W$.

5.4 Structure Function Uncertainties

The uncertainties in the structure function parameterization directly affect the extraction of $\sin^2\theta_W$ and ρ through the corrections calculated with the Monte Carlo. The errors associated with the strange, non-strange, and charm sea along with the charm quark mass will be discussed in the following Section. Here, we describe the errors associated with two other areas: 1) the longitudinal structure function and 2) other higher twist contributions to the structure functions.

Measurements [28] of the longitudinal structure function F_L or, equivalently, of $R = \sigma_L/\sigma_T$ are predominantly in the low Q^2 region ($Q^2 < 30GeV^2$). This precludes any precision comparisons of perturbative QCD predictions with the F_L measurements because the measurements are dominated by "higher twist" contributions. Nevertheless, the cumulative data (SLAC, CDHSW, BCDMS, EMC) are sufficiently precise to permit an empirical parameterization of F_L with approximately 20% precision. This parameterization of the F_L measurements is to be used in the neutral current analysis and the 20% uncertainty translates into a small error on $\sin^2\theta_W$, less than .0001.

Higher twist contributions to the structure functions can change the predicted ratios of neutral to charged current events. These higher twist processes fall as $1/Q^2$ relative to the leading hard-scattering mechanism and have typically been assumed to have a NC/CC

ratio similar to the leading contribution. For these reasons, the higher twist contributions have been neglected in previous analyses. Recently, Pumplin[29] has inferred using a vector dominance (VDM) calculation that these higher twist contributions could be much more important. On the other hand, recent analyses of the Q^2 dependence [30] of the combined SLAC and BCDMS F_2 structure function measurements, limit these possible higher twist contributions and indicate that the VDM process is highly suppressed. With this suppression, the VDM process will introduce only a small uncertainty in R_ν of less than 0.10% or less than .0005 in $\sin^2\theta_W$.

5.5 Non-Strange and Charmed Sea

Uncertainties in the $\bar{u}$ and $\bar{d}$ sea quark distributions and the possibility of a non-zero charmed quark sea introduce very small theoretical errors in R_ν, $R_{\bar{\nu}}$, and R^-. The $\bar{u}$ and $\bar{d}$ uncertainties are almost completely eliminated through the use of the Llewellyn Smith formula; they are removed through the measurement of the quantity r. A variation of the $\bar{u}+\bar{d}$ sea by 10% relative to the $u+d$ distributions, based on measurements of deep inelastic muon scattering on hydrogen and deuterium targets by the BCDMS [31] and NMC [32] collaborations, affects $\sin^2\theta_W$ by 0.04%. The presence of a $c\bar{c}$ sea at the level of 0.05 ± 0.05 of the strange sea, based on searches for wrong sign single muons [33], causes the same error on the weak mixing angle.

6 Other Physics Topics for Phase I

6.1 Exclusive $\nu_\mu \rightarrow \nu_e$ Oscillation

Neutrino oscillations provide a sensitive probe to neutrino masses, lepton mixing, and CP-violation in the lepton sector. If neutrinos were massive and had non-zero coupling between different flavors, then the weak neutrino eigenstates become linear combinations of mass eigenstates, which induces a flavor oscillation. The oscillation is a function of two parameters: Δm^2, a function of the neutrino masses, and $sin^2(2\alpha)$ where α is a mixing angle. The simplest treatment of this phenomenon encompasses oscillation between two species. If a neutrino were produced in a pure weak eigenstate (e.g. $\pi^+ \rightarrow \mu^+ + \nu_\mu$), the probability that it would have oscillated into a neutrino of different flavor (e.g. ν_e) is given by:

$$P(\nu_\mu \rightarrow \nu_e) = \sin^2(2\alpha)\ \sin^2(1.27\Delta m^2 L/E_\nu),$$

where $\Delta m^2 = m_1^2 - m_2^2$ where m_1 and m_2 are the masses of the two species in eV^2, L is the flight path in kilometers, E_ν is the neutrino energy in GeV, and $sin^2(2\alpha)$ connotes the "mixing probability" for large Δm^2. The flavor oscillation of neutrinos could be studied either by searching for the anomalous appearance of ν_a type neutrinos in a beam of predominantly ν_b type neutrinos (the exclusive oscillation), or by measuring the change in flux of a given neutrino type, ν_b, with distance and energy (the inclusive oscillation). The best sensitivities in the mixing angle come from the exclusive oscillation searches.

A high statistics SQT experiment offers an attractive venue to search for exclusive $\nu_\mu \rightarrow \nu_e$ oscillations. With the proposed statistics of this experiment, we expect to extend the limit of the mixing angle, $\sin^2(2\alpha)$ by a factor of five: $\sin^2(2\alpha) \leq 7 \times 10^{-4}$ for $\Delta m^2 \geq 10 eV^2$. This experiment will be sensitive to Δm^2-regions that are pertinent to the "closure question" of the universe. The closure hypothesis is: if massive neutrinos (ν_μ or ν_e) constitute the missing dark matter, then for the universe to be closed, the mass of one of the species should

be $20eV \leq m_\nu \leq 100eV$. Such a mass would imply that we should search in the region $\Delta m^2 \geq 400eV^2$.

The basic method to search for $\nu_\mu \rightarrow \nu_e$ oscillation in our SQTB experiment is as follows. We propose to look for very high energy electromagnetic showers in our detector. Under the oscillation hypothesis, these events would come about from low hadron energy ν_e charged current events; the ν_e's themselves appear due to the flavor oscillation of ν_μ's. These events would contrast sharply from the ordinary ν_μ-induced neutral current events in having large energies and having a small η_3 (see Section 4.1). Fig. 22 shows the η_3 distributions of neutral current and charged current events with calorimetric energy greater than 200 GeV; these distributions are compared to an EGS prediction of a pure electromagnetic shower of equivalent energy. There is a finite background from the contaminant ν_e's from three body kaon decays. The amount of this contamination relative to ν_μ is small for $E_\nu > 200GeV$ (see Fig. 23). Furthermore, as discussed in Section 4, the contaminant ν_e could be estimated with a systematic precision of $\leq 2\%$. For the oscillation analysis, we intend to determine the ν_e background using the ν_μ charged current data and check it against a beam Monte Carlo.

We present below a calculation for the exclusive $\nu_\mu \rightarrow \nu_e$ oscillation that incorporates conservative cuts to minimize the background. We commence by imposing a total visible energy cut of 250 GeV on events with no visible muon tracks. The expected number of neutral current events including CC contamination for the sample is 690 events. The corresponding number from the ν_e contamination is expected to be 30 events. The ν_e background, coming from the three body decay of the kaons, would be uniformly spread over the detector whereas the ν_μ-induced events would be clustered at the apparatus centre. Imposing a radius cut of 76 cm, reduces the background by 64%, in contrast to a corresponding loss of 20% for the signal. Finally, by imposing the η_3 cut the expected neutral current background is reduced to 55 events; the surviving ν_e background is about 8 events. The expected denominator, assuming full mixing, is 37,817 events after cuts. The calculation is detailed in Table 9. Thus, the expected sensitivity for the probability for $\nu_\mu \rightarrow \nu_e$ oscillation is:

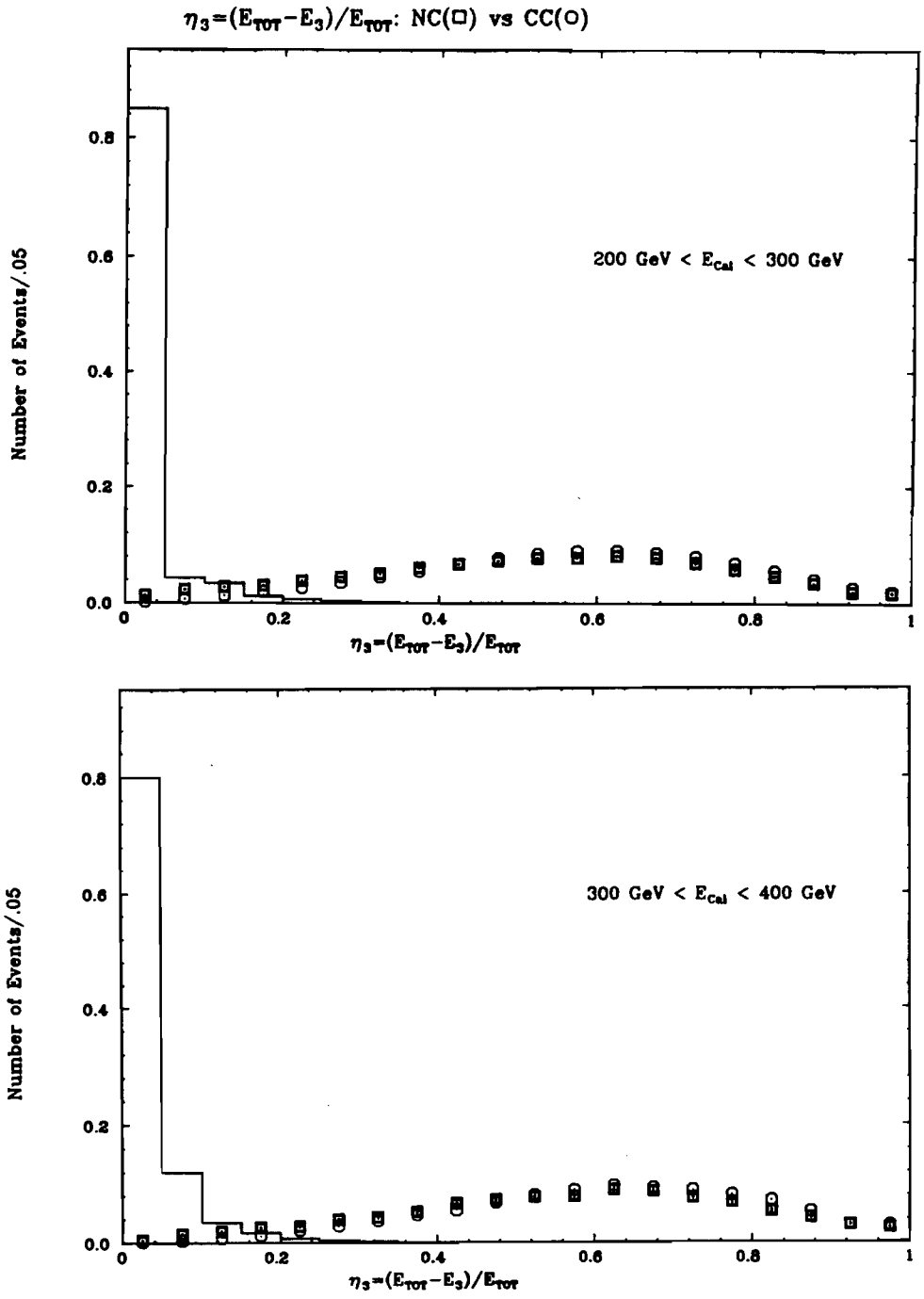

Figure 22: η_3 distributions for 200 GeV < $E_{\text{calorimeter}}$ < 300 GeV and 300 GeV < $E_{\text{calorimeter}}$ < 400 GeV. Symbols represent neutral current and charged current events from the E744/E770 Quadrupole Triplet runs. Solid lines represent an EGS prediction for pure electromagnetic showers

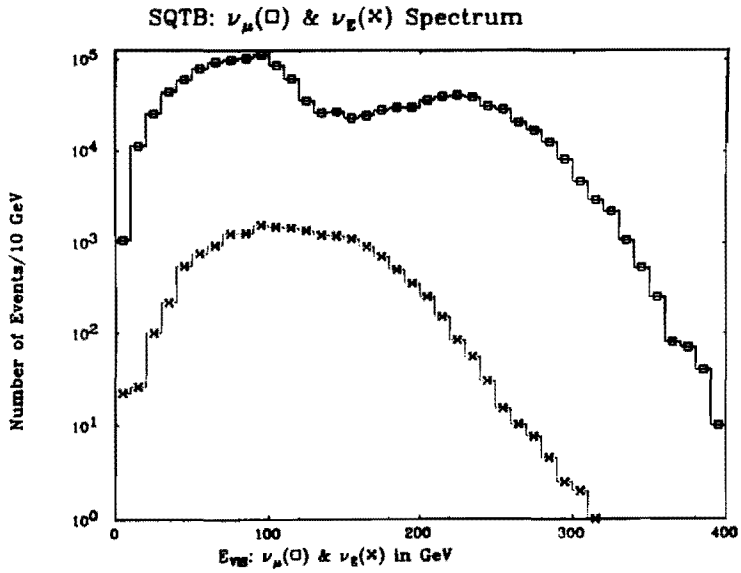

Figure 23: Predicted ν_e and ν_μ Energy Spectra for the SQT.

$$P(\nu_\mu \rightarrow \nu_e) = 3.4 \times 10^{-4} \text{ 90\% CL}$$

The above probability leads to a limit on the mixing angle of $sin^2(2\alpha) < 6.8 \times 10^{-4}$ for $\Delta m^2 \rightarrow \infty$. The region we expect to be sensitive to for this exclusive oscillation is pictured in Fig. 24 and compared to the presently available limits.

The above calculation is conservative and could be improved with the real data by exploring other regions and investigating various cuts to maximize our sensitivity to this process.

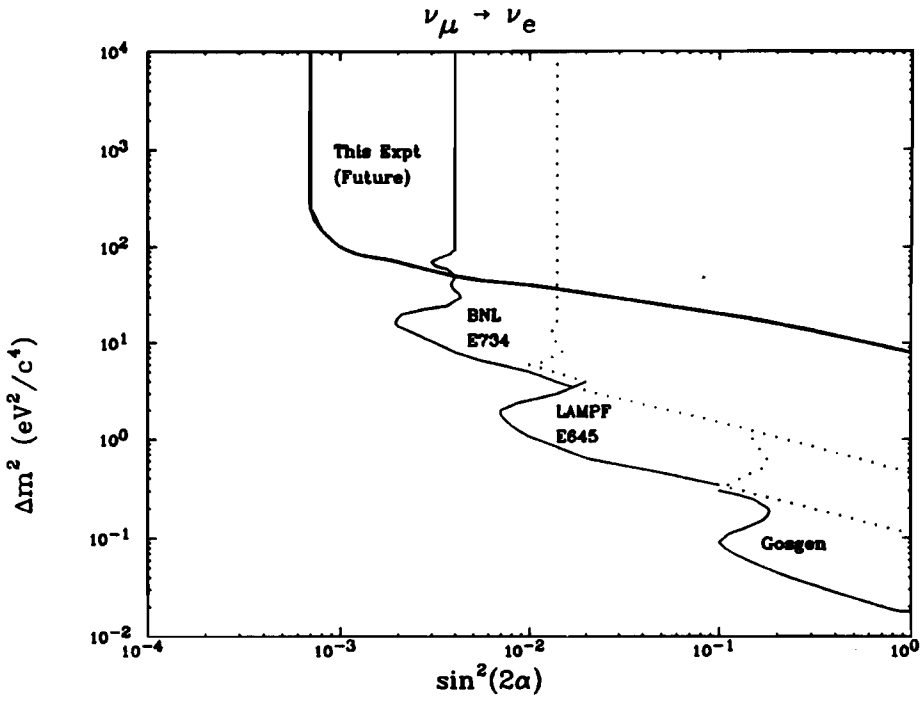

Figure 24: Limits on the Exclusive Oscillation $\nu_\mu \rightarrow \nu_e$

Table 9: Number of events for ν_μ-induced NC events (with CC contamination), ν_e-induced events, and expected signal for ν_e as a function of cuts.

Cuts	ν_μ-NC	ν_e	Signal
Radius< 1.27m	690	30	67530
Radius< 0.76m	552	11	54024
$\eta_3 < \eta_{CUT}$	55	8	37817

6.2 Study of Wrong-sign Single Muon Production

A high statistics SQTB experiment is a unique laboratory to study the production of wrong-sign single muon (WSM) production. In a WSM event the charge of the muon in the final state, and hence its lepton number, is opposite to the one expected from the lepton number conservation:

$$\nu_\mu + N \rightarrow \mu^+ + X,$$

where X refers to hadron. A definitive excess of WSM over known backgrounds would indicate new physics. Possibilities include:

(1) Lepton number violation: if lepton number is not strictly conserved (possible reasons include neutrino oscillations or the existence of Majorana neutrinos) ν_μ interactions could produce WSM at the lepton vertex.

(2) Charmed component of the nucleon sea: if the nucleon sea has a non-zero charmed component, the ν_μ will interact with it via Z^0 exchange, $\nu_\mu + c \rightarrow \nu_\mu + c$. In the subsequent hadronization of c into a D-meson, then its semileptonic decay would give rise to a μ^+ in the final state.

(3) Flavor changing neutral current: if a valence u-quark could be converted to a charmed quark *via* a NC interaction, the μ^+ might come about from the prompt decay of the charm quark.

The physics interest in WSM sketched above motivates a study of this process in a neutrino beam with high flavor purity. The proposed SQTB would deliver a ν_μ beam with little $\overline{\nu}_\mu$ contamination, and it is in the neutrino run that we intend to study WSM production. The figure below (Fig. 25) compares the spectrum due to ν_μ CC events with the background spectrum due to $\overline{\nu}_\mu$ CC events; the level of contamination is very small.

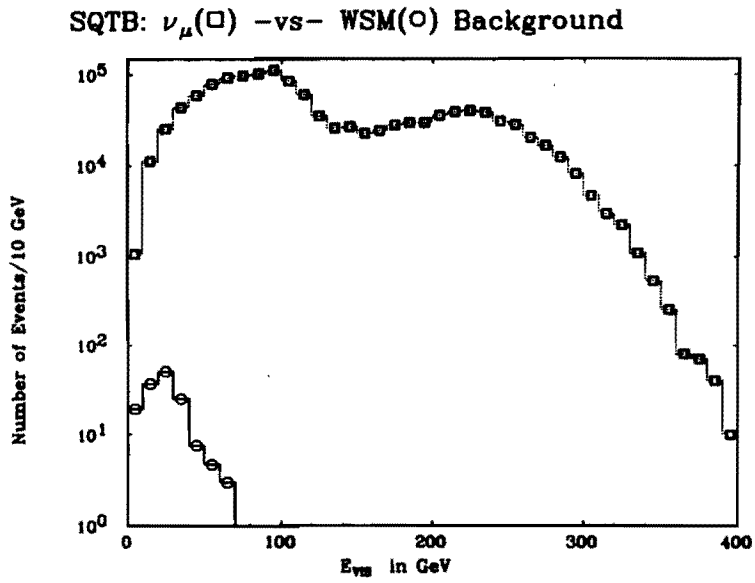

Figure 25: SQT Energy Spectrum for ν_μ CC events and $\bar{\nu}_\mu$ CC events

Two types of backgrounds affect the study of WSM. These are (a) contaminant $\bar{\nu}_\mu$-induced charged current interactions, and (b) ν_μ- or ν_e-induced interactions where the leading lepton remains invisible. The second type of WSM background comprise ν_μ-induced $\mu^-\mu^+$ events where the μ^- either ranges out in the hadron shower or exits before being detected, ν_μ-induced neutral currents where a π^+/K^+ hadron in the shower decays to produce a μ^+ in the final state, and ν_e-induced $e^-\mu^+$ events where the electron is hidden in the shower. It follows that $\bar{\nu}_\mu$ initiated background would show a soft energy distribution (Fig. 25) and a characteristic soft y-distribution, whereas Type (b) background would predominantly populate a high-y region. To reduce sharply the $\bar{\nu}_\mu$ contamination, we propose to study the WSM production with $E_{VIS} > 100$ GeV only. Furthermore, since the two types of backgrounds display very different y-distributions, we shall study the WSM production with a $y < 0.5$ cut as well. Table 10 enumerates these backgrounds for an SQTB run with 10^{18} protons on the target. The Table indicates that we should be sensitive to the following WSM rate with respect to the ordinary ν_μ CC events:

Table 10: Background to WSM with $E_{VIS} > 100$ GeV: Number of events due to $\overline{\nu}_\mu$-induced CC, ν_μ-induced $\mu^-\mu^+$, ν_e-induced $e^-\mu^+$, and ν_μ-induced NC where a μ^+ emerges in the final state, and the ν_μ-CC

Cuts	$\overline{\nu}_\mu$-CC	$\nu_\mu\ \mu^-\mu^+$	$\nu_e\ e^-\mu^+$	ν_μ-NC	ν_μ-CC
No y-cut	2.9 ± 0.8	31.1 ± 6.8	22.8 ± 4.6	27.3 ± 6.1	586321
$y < 0.5$	2.3 ± 0.7	2.3 ± 0.5	1.7 ± 0.3	2.1 ± 0.4	333435

$$\frac{\sigma(\nu_\mu \to \mu^+)}{\sigma(\nu_\mu \to \mu^-)} < 3.9 \times 10^{-5} \quad \text{No y-cut}$$

$$\frac{\sigma(\nu_\mu \to \mu^+)}{\sigma(\nu_\mu \to \mu^-)} < 1.5 \times 10^{-5} \quad \text{y} < 0.5$$

The statistical power of an SQTB run makes these sensitivities an order of magnitude better than those available from our earlier narrow band beam study.[33]

7 Outline of Phase II Program

7.1 Phase II Goals and Plans

The Phase II program of our proposal would realize the full potential of the new neutrino initiative. It would herald a next generation of deep inelastic neutrino physics programs,[34] sharpening tremendously the composite view of the Standard Model that neutrino interactions convey. The statistical sample of the Phase II experiment would comprise, after fiducial and kinematic cuts, 15×10^6 ν_μ-CC and 5×10^6 $\bar{\nu}_\mu$-CC events, and a corresponding increase in the neutral current and dilepton samples (see the Table below). The physics goals[35, 36] of the Phase II program are:

- Precision measurement of nucleon structure functions and subsequent tests of perturbative QCD predictions and determination of the strong coupling constant, α_S.

- Continued improvements in the measurements of the electroweak parameters to attain the desired goal of $\delta(\sin^2\theta_W) = 0.0015$ and $\delta(\rho) = 0.0025$.

- Sensitivity to exclusive $\nu_\mu \rightarrow \nu_e$ oscillations with mixing angles
$\sin^2(2\alpha) \leq 2 \times 10^{-4}$.

- Search for exclusive $\nu_\mu \rightarrow \nu_\tau$ oscillations.

- Search for right handed currents with the parameter $\eta^2 = |g_R/g_L|^2 < 0.0003$.

- Enhanced sensitivity for the searches of new phenomena and rare processes uniquely accessible via neutrino interactions.

We outline below some of these physics goals, dwelling primarily upon the need and the *sui generis* contribution of neutrino interaction to these areas, and sketch the research and development issues for the new apparatus. We hope to conduct the crucial R & D tests in Phase I.

Table 11: The Proposed Statistical Sample in Phase II. Number of $\nu(\bar{\nu})$-induced charged current (CC), neutral current (NC), and charm-induced opposite sign dimuon ($\mu^-\mu^+$) events in the new experiment, are presented below.

Experiment	ν_μ-CC	$\bar{\nu}_\mu$-CC	NC	$\mu^-\mu^+$
E744 + E770	1.4×10^6	0.3×10^5	0.4×10^6	1×10^4
New Experiment	15×10^6	5×10^6	5×10^6	15×10^5

7.2 Structure Functions and QCD

Precision tests of perturbative QCD, and "the best way" of achieving them, is a subject of some controversy arising largely due to the uncalculable contributions from "nonperturbative" effects.[37, 38] Nevertheless, within the framework of deep-inelastic experiments, there exist elegant and unambiguous predictions that could be directly tested against measurements. To quote G.Altarelli,[37] "In principle, deep inelastic leptoproduction is the most solid and powerful method for testing perturbative QCD and measuring α_S".

Two compelling tests of QCD within deep inelastic experiments are the evolution of structure functions with Q^2 at fixed x and the dependence of R (σ_L/σ_T) on x and Q^2.[35]

The evolution of the parity violating structure function xF_3 (the nonsinglet structure function) is the simplest. It is free of the details of gluon densities or the knowledge of R and therefore provides the cleanest channel for testing the Q^2 evolution predicted by the theory. We emphasize the uniqueness of testing the Altarelli-Parisi equation via xF_3 evolution:[39] $\partial ln(xF_3)/\partial ln(Q^2)$ at a given x is directly proportional to the strong-coupling constant, $\alpha_S(Q^2)$, up to the reliably known integral of the splitting function, ***without*** the complications of gluon and R evolution. The new CCFR QTB-data[35] demonstrate, for the first time, the Q^2-evolution of xF_3 consistent with the Altarelli-Parisi equation. The statistical and systematic precision of the earlier measurements of xF_3 in the narrow band

beam data of CCFR[40] and the wide band data of CDHSW[41] were such that the test of evolution equation was inconclusive.[38]

The next goal for QCD tests is a demonstration of $R_{EXPT} = R_{QCD}$. Fortunately, perturbative QCD predicts the absolute magnitude and shape of $R(x, Q^2)$ which can then be confronted in an deep inelastic scattering experiment.[42] Nevertheless, it has been pointed out that the current deep inelastic muon and neutrino data are *consistent* with but *do not demonstrate* $R_{EXPT} = \sigma_L/\sigma_T = R_{QCD}$.[43] Precision measurements of R, viable with 20 million neutrino and anti-neutrino events with commensurate systematics, will singularly confront the theoretical prediction.

Evolution of the singlet structure function, F_2, and the subsequent extraction of the gluon densities will provide an adequate system of tests of QCD following the two forementioned tests. The statistical precision and the envisioned systematic improvements of Phase II should yield an error on Λ_{QCD} of ≤ 15 MeV. Such a precision might permit a measurement of the running coupling constant of the strong interaction.[44] We also point out the power of neutrino scattering in achieving an unambiguous gluon structure function: since neutrino-quark scattering is flavor selective, when F_2 and xF_3 are evolved simultaneously, the in-built ability to constrain anti-quarks densities results in a superior determination of the gluon structure function.

The statistical strength of the new experiment permits the extraction of quark and antiquark distributions separately for neutrinos and antineutrinos; and thus test the hitherto untested, ubiquitous universality assumption, of the standard model regarding quark densities. This assumption at present cannot be tested due to the paucity of antineutrino events. Furthermore, the only direct measurement of the strange sea comes from a study of neutrino induced opposite sign dimuon events.[45] The 150,000 opposite sign dimuons in Phase II will give an unprecedented handle on the strange sea density including its Q^2 evolution. Structure functions with $x > 1$ have been topics of speculation as well. The primary limitation of statistics and of resolution smearing could be effectively alleviated in a new experiment;

and new territories could be explored. Finally, the traditional quark-parton model integral tests, such as Gross-Llewellyn Smith sum rule and the mean square charge test, could be performed with a much better accuracy.

The normalization of data, both absolute and relative, can be achieved in this experiment. The absolute normalization of neutrino data could be determined using the inverse-muon decay events — a process of unambiguous theoretical prediction and of interest in its own right. Antineutrino data are tied to the neutrino data by extrapolating $d\sigma/dy$ to $y = 0$.Presently, this process is measured at a 5.7% level,[46] statistics being the dominant uncertainty. An accuracy of 1% should be achievable at the new experiment. For the QCD tests, however, only the energy-to-energy and neutrino-to-antineutrino normalization (the relative normalization) matters. This could be determined in a variety of ways and have been addressed by the CCFR collaboration.[47]

7.3 Improvements in the Electroweak Parameter $\sin^2\theta_W$

The Phase II of our neutrino experiment would attain substantial improvements over the electroweak parameters that will be measured in Phase I. Improvements in $\sin^2\theta_W$ could be attained in a QTB where we eliminate or alleviate the present limitations of this beam; improvements in the ρ measurement on the other hand would require an SQT run with the new apparatus. The key to achieving this is to determine $\sin^2\theta_W$ among statistically exclusive kinematic regions of ν-N event sample such that systematically, too, these are as independent as possible.[35] This is achievable in a high statistics experiment with suitable instrumentation.

First, we deem it feasible to measure experimentally R_ν to $\leq 0.35\%$ accuracy by the amelioration of the two principal contaminations in the determination of this ratio:

(a) Short charged current events: these decrease almost proportionately with increasing neutrino energy; thus at the Tevatron these should be about half of those estimated at past

experiments. Furthermore, a large fraction of these events (given average neutrino energy $\approx$ 150 GeV) are "exiting muons" leaving the detector at large angles. Improved pattern recognition with finer segmentation (e.g. transversely segmented scintillation counters and drift chambers every 2" of steel) could alleviate this background substantially.

(b) Electron neutrino contamination: In order to manage this background, it is necessary to measure directly the poorly determined K_L-induced ν_e's in the detector (present in a QTB experiment). We hope to measure the unknown K_L background in a QTB running during Phase II. We are investigating the idea of bending the charged particles from the beam path; the remaining neutral K_L would produce neutrino interactions in our detector which then could be normalized to the number of incident protons. We will also try to improve our measurement of the low-hadron energy ν_e's directly in the apparatus. Once again, the proposed finer segmentation in calorimetry (scintillation counters every 2" of steel) would enable a clean differentiation between an electromagnetic (low hadron energy ν_e) and a hadronic shower.

Secondly, the dominant theoretical limiting factor to $\sin^2\theta_W$ determination from R_ν, the uncertainty in the mass-parameter of the charm quark (m_c), could be obviated in a variety of ways in Phase II.

- If we apply a correlated cut on the hadronic energy of the events and the angle of hadron shower then R_ν is virtually insensitive to m_c.

- Additionally, using the 150,000 $\mu^-\mu^+$ events, we should substantially reduce the current error on m_c.

- Thirdly, by using an improved measurement of the semileptonic branching ratio of the charmed hadron, we could try to "subtract" directly the charm component of the charged current sample in the denominator of R_ν.

- Finally, the possibility of measuring the inverse muon decay process to about 1% accuracy

opens the possibility of normalizing the neutral current with respect to ν_μ-e scattering. This method of extracting $\sin^2\theta_W$ is independent of the traditional theoretical concerns when using charge currents to normalize the data (e.g. charm mass, strange-charm asymmetry, radiative correction error from W-γ box diagram etc.).

Thus, in a Phase II experiment we will deal with a system of tests to measure $\sin^2\theta_W$ and, by collating and contrasting the independent or almost independent systematic errors, we will arrive at the desired precision of 0.0015 in $\sin^2\theta_W$. To conclude this section, we point out the feasibility of remeasuring $\sin^2\theta_W$ via the Paschos-Wolfenstein technique by performing a high statistics sign selected run with the improved injector. As discussed earlier, a determination of $\sin^2\theta_W$ using this relation is largely insensitive to many theoretical and experimental limitations, and thus provides an additional check on the prior determination of this quantity.

7.4 The Exclusive $\nu_\mu \rightarrow \nu_e$ Oscillation

We will continue improving our $\nu_\mu \rightarrow \nu_e$ oscillation search begun in Phase I. If we have measured the K_L component of the QTB beam in Phase II, we will have a reliable estimate of the ν_e contamination in our beam ($< 2\%$). This would then enable us to have the statistical power of the QTB beam, with well-controlled systematics. With these assumptions, an estimate of the limit on the oscillation angle yields:

$$sin^2(2\alpha)[\nu_\mu \rightarrow \nu_e] < 2 \times 10^{-4} \text{ @ 90 \% CL: Phase II}$$

7.5 Rare and New Physics

The statistical power of the new experiment offers a wide vista for measuring, with superior accuracy, rare processes with rates $\leq 10^{-6}$ of the regular charged currrent events, and for

searching for new phenomena. We enumerate some of these below.[48]

i. **Inverse Muon Decay:**[49] The purely leptonic reaction, $\nu_\mu + e^- \rightarrow \mu^- + \nu_e$, offers an elegant test of the standard model. We could learn the structure of the Lorentz current of the weak interaction, the scalar coupling of leptons, as well as the energy dependence of its cross section. It offers an absolute normalization of ν-events.

ii. **Measurement of V_{cd}:**[45] Opposite sign dimuons offer the only direct means of measuring the Cabibbo-Kobayashi-Maskawa matrix element. The present measurements could be vastly improved.

iii. **Recoilless Dimuons:** Measurement of the destructive interference between the neutral current and charged current channels of neutrino scattering off the coulomb field of the nucleus (the so called ν-induced trident events) directly tests the gauge structure of the standard model. In the new experiment in excess of 600 trident events will be observed.

iv. **Neutral Heavy Leptons:** Neutrino experiments are sensitive to iso-singlet type neutral heavy leptons (as opposed to sequential fourth generation neutrinos). For low mass neutral heavy leptons (< 5 GeV), the sensitivity in the new experiment will be far superior to the e^+e^- experiments. By instrumenting the apparatus suitably, we could extend the search domain with masses down to 10 MeV and with coupling suppressions down to 10^{-9}.

vi. **Search for Right Handed Currents:**[50] The y-distributions of neutrino and antineutrino CC events constrain the right handed currents in the most model independent way. The current limit on the mixing of the right handed currents from the CCFR(QTB) experiments is the most stringent one. The corresponding limit from the muon-decay are sensitive to the theoretical assumptions such as the mass of the right handed neutrino. In

the new experiment the derived limit on the mass of the right handed boson should be the most stringent.

vii. Like Sign Dimuons: With a sample of over 2000 like sign dimuons, we should be able to test the QCD prediction of like sign dimuon production, something that has proven elusive till now.

viii. Trimuons: Neutrino-induce trimuons predominantly arise from hadronic sources (vector meson resonances). The new sample should have over 1300 of these events; offering an opportunity to do a quantitative test of various hypotheses.

7.6 Beam and Detector Requirements

The most compelling need to achieve the physics goals sketched above is of an intense neutrino beam at as high an energy as possible. The increase in the luminosity of an order of magnitude with respect to the previous quadrupole triplet beam could be accomplished with the new Linac and the improved Main Injector at Fermilab. Discussions above show that high statistics is the primary requirement to realize the physics objectives in Phase II. An increase in the neutrino energy, which is directly related to the primary energy of the proton, would help *enormously* for conducting QCD tests, measuring $\sin^2\theta_W$, and exploring the physics of rare processes.

The detector, to be commensurate with the statistical power of the new experiment, will have to be such as to permit the desired tests and achieve the necessary precision. To this end, two major upgrades of the detector capability are required. First, the systematic measurement of momentum has to be improved by a factor of twenty. This would imply instrumenting an air-core spectrometer.[51] It should be borne in mind that an iron toroidal magnet cannot furnish momentum resolution better than 8-9 % due to multiple coulomb

scattering. With this resolution, it seems very difficult to achieve a systematic accuracy of the order stated above. Second, the sampling calorimeter has to be improved significantly. This is crucial for reliable hadron energy measurements, improving pattern recognition, and reducing the background in the neutral current analysis. Some of these parameters and components of the new apparatus have to be investigated in detail and we have begun this process. There are, however, a few specific improvements that we deem imperative. We expect to study these in a test run during Phase I running as outlined below.

8 Requirements

8.1 Phase I Detector (Lab E) Recommissioning

In order to reestablish the Lab E facility as a working neutrino experiment, we would require PREP electronics, a new data acquisition computer, rigging to reconfigure the detector, and labor and materials to recondition the existing drift chambers and target cart systems. Much of the Lab E PREP electronics used in E744/E770, including the LeCroy Fera ADC system, has been redistributed to experiments that were active in the 1990 running period. These electronics would have to be replenished either from the existing pool or purchased new.

The Lab E data acquisition system (PDP-11, Vax 780 and associated peripherals) has also been returned and is no longer available. We would use our experience, as well as the advice of the Computing Department, to design a replacement system that would satisfy Phase I needs but would be flexible for future Phase II requirements. One possibility is to use a microvax plus a small number of ACP cards to collect and write data to tape.

The Lab E experimental hall has been reconfigured for the HERA calorimeter tests. For neutrino running, the target carts and toroids would have be re-positioned, and the veto wall would have to be reassembled.

Based on our experience from the 1988 run of E770, both the drift chambers and scintillation counters will need to be reconditioned before data acquisition can take place. This includes checking the performance of individual phototubes and drift chamber cells, and making repairs as required. Additionally, dust and dirt has accumulated on the TDC electronics in the Lab E experimental hall. We plan to clean all of this electronics and rebuild the TDC crates to make them more hermetic and less susceptible to the outside environment.

We also need to perform a modest upgrade to the TDC electronics. To fully exploit the

measurements of neutral current events, additional TDC channels are required. Furthermore, based on our E770 experience we wish to increase the memory capacity of each TDC.

8.2 Test Beam Requirements for Phase I and R&D for Phase II

Precision measurements of the electroweak parameters require a thorough understanding of the calibration of the apparatus. Whereas we shall be using a calorimeter that was well calibrated three years ago, the change of light output of the scintillation calorimetry with time requires a recalibration. Furthermore, the quest of greater precision in the $\sin^2\theta_W$ measurement has compelled us to consider measuring *in situ* the ν_e contamination of the beam by identifying the the low hadron energy ν_e-induced electromagnetic showers in our detector. This can be done reliably by measuring the electrons of known energy in our calorimeter – something we have not done so far. Equally important are the prototype developments and R & D investigations for Phase II. This would necessitate a well monitored test beam setup available to us during data taking.

8.2.1 Test Beam for Phase I

To measure the calibration constant for hadrons, we would need hadrons with a narrow momentum-bite at momenta of 40, 70, 100, 150 and 200 GeV to be delivered to us at Lab E. We intend to have a dedicated calibration run, sometimes in the middle of our data taking, for a period of two weeks. Using these test beam hadrons, we also intend to make an important background measurement relevant to the search for neutral heavy leptons in ν-N scattering. [52] The relevant process is the search for double vertices in ν-N scattering where presumably the neutral heavy lepton is sufficiently long lived to travel beyond the end of the first hadron shower and then decays in the detector. The background for this signal is the neutral hadron punchthrough in an ordinary neutral current event. In the test run, we could measure this background in our detector and subsequently enhance our sensitivity

for this exotic search.

Electromagnetic showers can be reliably simulated using the EGS Monte Carlo. Nevertheless, we intend to check the simulation against data in our apparatus with at least two different energies. The parameterization of the electromagnetic shower development then could be refitted and collated against the proposed measurements. We hope to accumulate electron data in our calorimeter at 40 and 100 GeV respectively. This should provide ample precision for the electromagnetic shower simulation in our detector.

8.2.2 Prototypes and R & D studies for Phase II

The ambitious upgrades of the scintillation and gas calorimetry for Phase II requires a new instrumented cart with the prototype detector elements. We hope to test two new elements under consideration for Phase II:

The new Scintillation Calorimeter

The new prototype scintillation calorimetry would consist of the following features:

• Improved longitudinal segmentation: Improvement in the hadron shower resolution and in distinguishing electromagnetic from hadronic showers requires finer segmentation. We intend to double our sampling from the present counter/4" of steel in Phase II.

• Transverse segmentation: Next, we need to improve upon the systematic precision of hadron energy measurement for the QCD study. At present the biggest correction to the hadron energy measurement is the correction for pulse height *vs.* position in the counter. This correction is almost 100% at the corners of the detector. To eliminate this correction we need transverse segmentation in the calorimeter (at present, there is no segmentation in the CCFR counters).

• An equally important motivation for transverse segmentation is an ability to tag an exiting

muon in a CC event; these short CC events are responsible for one of the largest experimental systematic errors in determining $\sin^2\theta_W$. The elimination of these exiting muons will decrease the experimental error from this source by more than a factor of two.

• An added bonus of this improvement will be a marked improvement in the time-resolution of neutrino-induced events, which in turn will help searches for rare processes.

We propose to build a new cart with twenty-eight 10'×10' steel plates, interspersed with polystyrene-based scintillation counters. Each counter will be transversely segmented into eleven strips. The outmost two strips will be 10'×6" each. The inner nine strips will be 10'×1'. Each strip will be instrumented with one phototubes at each end. We expect to instrument the new cart with 28 such counters and take test beam hadrons concomitant with neutrino running. We shall quantify improvements in the resolution and systematics of of hadron energy measurement, electron-to-hadron separation, and event time resolution.

Improved Gas Calorimetry

We would like to measure the transverse momentum of the hadron shower in a neutrino interaction with high precision in Phase II. The salient reasons for doing so are the following:

• We need the hadron shower angle measurement to search for exclusive $\nu_\mu \rightarrow \nu_\tau$ oscillations. Our objective is to search for ν_τ-induced τ lepton which then subsequently decays into muon and two neutrinos. These events, having two neutrinos in final state, will be marked by large missing transeverse momenta (P_T). By measuring the angle of the hadron shower one could measure the missing P_T. The ordinary CC events by contrast would have zero or small missing P_T. Our goal is to measure the angle of a 100 GeV hadron shower with an rms resolution of less than 10 mrad.

• We need the hadron shower angle measurement to eliminate the mass of the charm quark uncertainty from the electroweak parameter determination. By imposing cuts on this angle it should be possible to cut out events which are at low-Q^2 and most susceptible to this

uncertainty.

• We need the hadron shower angle to monitor the calibration systematics. The hadron shower angle measurement provides an extemely important check on the systematics of the CC events. It will be a redundant measurement and thus provide us with a continuous monitoring of calibration which will prove to be invaluable.

The FADC's of the Lab E drift chamber can be used for this measurement. However, the resolution with the current sampling may be inadequate for Phase II studies. We need to measure the resolution function of the angle measurement with high statistics test beam data. One of the questions we intend to answer is whether we could reach a hadron angle resolution of 5 mrad. We shall measure the angle of the hadron shower with our 3-wire drift chambers (borrowed from our neutrino target) and flash ADC's in the new cart. In the past, with a drift chamber every 8" of steel, our calorimeter has yielded an rms resolution of about 20 mrad at 100 GeV. This needs to be improved dramatically. Since this test would require 28 drift chambers we shall have to interrupt the regular neutrino data taking for a couple of weeks to instrument the new cart.

8.3 Costs and Requests

The major costs to the laboratory for Phase I would be the recommissioning of the Lab E facility, prototype development for Phase II, and the construction of the Sign-Selected Quadrupole Triplet beam line. These costs are estimated in the table below.

The recommissioning of Lab E will include the reconditioning of existing drift chambers and scintillation counters, repositioning of target carts, reconstruction of the veto wall, refurbishing of the data acquistion system and reacquisition of PREP electronics. These costs are delineated in the table below. Note that the PREP electronics estimate is based on a 1988 inventory in which the total cost of all Lab E prep electronics was $893K. We assume a 20 percent increase in cost with 1990 US dollars plus an additional 20 percent for electron-

ics upgrades. We also include expenses associated with reactivation of the drift chambers, scintillation counters, and associated electronics.

A new target cart with 2 inch segmentation will be the major detector prototype for Phase II. We include our best estimates for raw materials and labor. Scintillator estimates are based on 2800 ft^2 of scintillator at \$70/ ft^2, and 616 channels of phototubes and electronics (including ADCS) at \$100/channel. We include an additional \$100K for miscellaneous equipment such as cables and connectors and tools.

Finally, we include an estimate for the cost of the new sign selected beam line. The beam line design utilizes many existing elements (4Q120's and Eartly Dipoles) along with the enclosures from the Quadrupole Triplet beam line. The biggest expenses will be associated with modifying two of the existing dumps and reconfiguring the pre-target region.

In order to carry out Phase I of this program we will need manpower resouces comparable to that realized in E744/E770. Our goal is to have have 8 faculty-staff, 5 postdocs , 8 graduates students and 2-3 technicians from a total of 5 institutions. At present, there are 8 faculty-staff and 1 postdocs from 3 institutions committed to this experiment. We also anticipate that 2 Physics Department technicians that were assigned to E770/E744 will be reassigned to P815. These technicians are thoroughly familiar with our present drift chamber and scintillation counter system, and proficient in scintillation counter construction.

Table 12: Cost Estimates for P815 Upgrades (1990 US Dollars)

Item	Costs
Lab E Recommission	
PREP Electronics	1250K (new + existing)
Data Acquisition Computer	100K
Reconstruction of Veto Wall	20K
Detector Realignment	20K
Recondition DC Electronics	20K
Recondition Drift Chambers	20K
Recondition Scint. Counters	20K
TDC Upgrades	40K
Target Cart Prototype for Phase II	
100 Tons of Steel	30K
Fabrication	70K
Scintillator	170K
Phototubes +Electronics	620K
TDC Electronics	20K
Cables + Misc. Expenses	100K
Sign Selected Quad Triplet Beam	300K
Total	2800K

9 Conclusions

A major physics objective of the 1990's will be precision tests of the electroweak sector of the Standard Model. Our understanding of this subject is such that the measurables in e^+e^- collisions at the Z^o pole, the hadron collider results, and deep inelastic neutrino-nucleon neutral and charged current scattering should all agree. A central issue is the role of the top quark, which in the Standard Model enters in the propagator and vertex electroweak corrections for all processes beyond the tree level. Given the comprehensive foundation of the Model, precise experimental data will incisively confront the theory.

Our proposal will exploit the full power of the high energy and intensity of the Tevatron neutrino beam to significantly improve the precision of the electroweak parameters determined in deep-inelastic neutrino-nucleon scattering. With a sign-selected neutrino beam neutrino and antineutrino interactions can be separately measured and important systematic errors can be controlled.

The objectives of Phase I of our program are: (1) Measurement of $\sin^2\theta_W$ with an expected error of $\delta \sin^2\theta_W = \pm 0.0029$ (statistical and systematic errors combined). (2) Determination of ρ to a level of ± 0.0049 (statistical and systematic errors combined). (3) The search for neutrino oscillations, which will extend the range of the oscillation parameter $\sin^2 2\alpha$ by roughly an factor of five, and the search for wrong-sign muons, indicative of lepton number violation.

This level of precision on the electroweak parameters can be quantified by the restrictions imposed on the top quark mass, where we find $\delta m_t = \pm 30$ GeV/c^2. These limits will always be complementary to the determinations at electron and hadron colliders given the entirely different channels probed in deep-inelastic neutrino-nucleon scattering.

The proposed Phase I program can be conducted with modest expense to FNAL. The chief costs are the construction of the new sign-selected neutrino beam and the recommissioning

of the Lab E neutrino detector. We view Phase I of this effort as the initial stage of a comprehensive program of neutrino physics at FNAL in the 1990's. The Phase II program will extend the electroweak physics measurements and will probe QCD at a new level of precision.

References

[1] Final CDHS results are presented in A. Blondel *et al.*, Z. Phys. C45, 361(1990). For CHARM, see J. Allaby *et al.*, Z. Phys. C36,611(1985). CCFR results are in P.G. Reutens *et al.*, Phys. Lett. 152B, 404(1987). New results from FMMF were presented in R. Brock, DPF'90 (Houston, Tx.)

[2] M. Shochet *et al.*, CDF/D0C/CDF/PUBLIC/1152, (1990).

[3] A. Sirlin, Phys. Rev. D22, 971, (1980).

[4] The package is called SSTWR — see M. Peskin, SLAC-PUB-5210, (1990) for a description of the calculations.

[5] The top mass of 150 GeV is favored by present data — see for example V. Barger *et al.*, Phys. Rev. Lett. 65,1313 (1990).

[6] See the section on high energy e^+e^- physics in the upcoming proceedings from the 1990 DPF Snowmass Workshop for a discussion of LEP and SLC performance prospects.

[7] J. Rosner, EFI 90-18-Rev (1990).

[8] R.G. Stuart, Z. Phys. C34, 445(1987).

[9] C.H. Llewellyn Smith, Nucl. Phys. B228 (1983) 205.

[10] E.A. Paschos, L. Wolfenstein, Phys. Rev. D7 (1973) 91.

[11] R. Bernstein and A. Malensek, FNAL TM, to be published.

[12] H.W. Atherton, CERN 80–07. Also see A. Malensek, FN–341.

[13] E–731 Collaboration, private communication.

[14] A discussion of the experimental errors, concentrating on the charged current subtraction, can be found in R. Brock, Deep-Inelastic Measurements of $\sin^2\theta_W$, New Directions in Neutrino Physics at Fermilab, p. 57(1988).

[15] P.S. Auchincloss et al., Nevis Preprint 1394, to be published in Z. Phys. (1990).

[16] M.H. Shaevitz , ν 90 Conference, June, 1990, CERN.

[17] D. Allasia *et al.* CERN-PPE/90-103, July, 1990.

[18] W. H. Smith, Neutrino-90 Conference, CERN, June, 1990.

[19] A. DeRujula *et al.*, Nucl. Phys. B154,394 (1979).

[20] A. Sirlin *et al.*, Nucl. Phys. B189,422 (1981).

[21] C.H. LLewellyn Smith, Nucl. Phys. B208,27 (1982).

[22] I. Liede *et al.*, HU-TFT-83-45 (1983).

[23] D. Bardin *et al.*, JINR-E2-86-260 (1986).

[24] J.V. Allaby *et al.*, Z. Phys. C 36,611 (1987).

[25] A. Blondel *et al.*, CERN/EP 89-101 (1989).

[26] P.G. Reutens *et al.*, Z.Phys.C. 45,539 (1990).

[27] P.Z. Quintas *et al.*, Nevis-R-1427, PDF Workshop at FNAL (1990).

[28] S.R. Mishra and F.J. Sciulli, Ann. Rev. Nucl. Part. Sci. 39 (1989)259.

[29] J. Pumplin, Phys. Rev. Lett. 64 (1990) 2751.

[30] D. Harrach, ν 90 Conference, June, 1990, CERN.

[31] A. Benvenuti *et al.*, Phys. Lett. B237, 599, 1990.

[32] D. Allasia *et al.*, CERN-PPE-99-103, 1990.

[33] S.R. Mishra *et al.*, Z. Phys. C44, 187, 1989.

[34] The feasibility and implications of such an experiment was discussed at the workshop "Fermilab in the 1990's" at Breckenridge, "A 2^{nd} Generation Neutrino Deep Inelastic Scattering Experiment at FNAL Tevatron", by S. R. Mishra. A discussion is to appear in the conference proceedings of the above, ed. R. Brock and H. Montgomery *et al.*

[35] S.R.Mishra, "Probing Nucleon Structure with ν-N Experiments", Nevis Preprint # 1426; to appear in the proceedings of "Workshop on Hadron Structure Functions and Parton Distributions", Fermilab, Batavia, Ill, Apr(1990).

[36] S.R.Mishra, "Lorentz Strucuture of the Weak Current..."; Nevis preprint #1429; Presented at Neutrino'90, CERN, Geneva, Jun(1990); to appear in the conference proceeding.

[37] G. Altarelli, "Tests of QCD ", Ann. Rev. Nucl. Part., 39, 366 (1989).

[38] S.R.Mishra and F.Sciulli, "Deep Inelastic Lepton-Nucleon Scattering", Ann. Rev. Nucl. Part., 39, 259 (1989).

[39] G. Altarelli and G. Parisi, Phys. Lett. B26, 298(1977).

[40] E. Oltman, PhD thesis, Columbia University, Nevis-270, Apr(89); to be published.

[41] B. Vallage, PhD thesis, Saclay CEA-IV-2513, Jan(87); to be published.

[42] G. Altarelli and G. Martinelli, Phys. Lett. B76, 89(1978); M. Gluck and E. Reya, Nucl. Phys. B145, 24(1978).

[43] S. R. Mishra and F. Sciulli, Phys. Lett. B244, 341(1990).

[44] The quadrupole triplet beam data by CCFR (E744 and E770) are currently being analyzed. It should be pointed out that within the systematic precision of these neutrino

experiments (CCFR & CDHSW) the best error on the QCD parameter, Λ_{QCD}, could not be reduced below 70 MeV.

[45] C. Foudas *et al.*, Phys. Rev. Lett., (1990); For recent experimental results from CCFR, see M. Shaevitz in Proc. of Neutrino '90.

[46] CCFR: S.R.Mishra *et al.*, "Improved Measurement of Inverse Muon Decay at the Fermilab Tevatron", Nevis Preprint # 1424, May(1990); accepted for publication in Phys. Lett. B.

[47] CCFR: P. S. Auchincloss *et al.*, accepted for publication in Z. Phys. C.

[48] S. R. Mishra, "Rare Processes in ν-N Scattering", Proceedings of Neutrino'88, p.259, Boston(1988), ed's J. Schneps *et al.*, World Scientific, Singapore.

[49] CCFR: S.R.Mishra *et al.*, Phys. Rev. Lett. 63, 132(1989).

[50] CCFR: S.R.Mishra et al., "A Study of the Space-Time Structure of the Weak Current in ν-N Scattering"; Nevis preprint #1428; submitted to Phys. Lett. B.

[51] An air-core toroidal spectrometer is being considered by the Saclay-Munich group to conduct a second generation deep inelastic muon experiment. See, C. Guyot *et al.*, "A New Fixed Target Experiment for a Precise Test of QCD", to be published in Proceedings of "Fermilab in the 1990's", ed. R. Brock and H. Montgomery.

[52] S.R.Mishra et al., Phy. Rev. Lett.,59,1397(1987)